AD-A131 064 RESEARCH ON ALGORITHMS FOR ADAPTIVE ARRAY ANTENNAS(U) 1/1
STANFORD UNIV CA DEPT OF ELECTRICAL ENGINEERING
B WIDROW ET AL. MAR 83 RADC-TR-83-35 F30602-80-C-0046
UNCLASSIFIED F/G 9/5 NL

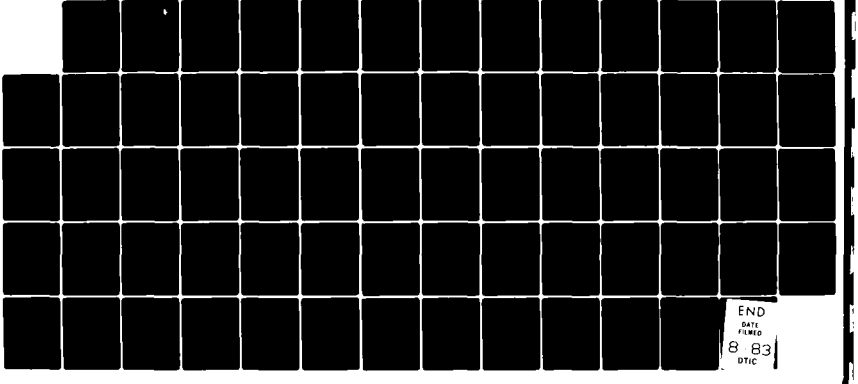

END
DATE FILMED
8 83
DTIC

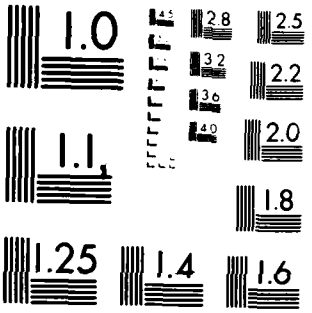

RADC-TR-83-35
Final Technical Report
March 1983

RESEARCH ON ALGORITHMS FOR ADAPTIVE ARRAY ANTENNAS

Stanford University

B. Widrow and R. Gooch

APPROVED FOR PUBLIC RELEASE; DISTRIBUTION UNLIMITED

ROME AIR DEVELOPMENT CENTER
Air Force Systems Command
Griffiss Air Force Base, NY 13441

This report has been reviewed by the RADC Public Affairs Office (PA) and is releasable to the National Technical Information Service (NTIS). At NTIS it will be releasable to the general public, including foreign nations.

RADC-TR-83-35 has been reviewed and is approved for publication.

APPROVED: John A. Graniero

JOHN A. GRANIERO
Project Engineer

APPROVED: B Beek

BRUNO BEEK, Technical Director
Communications Division

FOR THE COMMANDER: John P. Huss

JOHN P. HUSS
Acting Chief, Plans Office

If your address has changed or if you wish to be removed from the RADC mailing list, or if the addressee is no longer employed by your organization, please notify RADC (DCCD) Griffiss AFB NY 13441. This will assist us in maintaining a current mailing list.

Do not return copies of this report unless contractual obligations or notices on a specific document requires that it be returned.

UNCLASSIFIED

SECURITY CLASSIFICATION OF THIS PAGE (When Data Entered)

REPORT DOCUMENTATION PAGE		READ INSTRUCTIONS BEFORE COMPLETING FORM
1. REPORT NUMBER RADC-TR-83-35	2. GOVT ACCESSION NO. A131064	3. RECIPIENT'S CATALOG NUMBER
4. TITLE (and Subtitle) RESEARCH ON ALGORITHMS FOR ADAPTIVE ARRAY ANTENNAS		5. TYPE OF REPORT & PERIOD COVERED Final Technical Report February 81 - November 82 6. PERFORMING ORG. REPORT NUMBER N/A
7. AUTHOR(s) B. Widrow R. Gooch		8. CONTRACT OR GRANT NUMBER(s) F30602-80-C-0046
9. PERFORMING ORGANIZATION NAME AND ADDRESS Stanford University Department of Electrical Engineering Stanford CA 94305		10. PROGRAM ELEMENT, PROJECT, TASK AREA & WORK UNIT NUMBERS 61102F 2305J805
11. CONTROLLING OFFICE NAME AND ADDRESS Rome Air Development Center (DCCD) Griffiss AFB NY 13441		12. REPORT DATE March 1983 13. NUMBER OF PAGES 68
14. MONITORING AGENCY NAME & ADDRESS(if different from Controlling Office) Same		15. SECURITY CLASS. (of this report) UNCLASSIFIED 15a. DECLASSIFICATION/DOWNGRADING SCHEDULE N/A

16. DISTRIBUTION STATEMENT (of this Report)

Approved for public release; distribution unlimited

17. DISTRIBUTION STATEMENT (of the abstract entered in Block 20, if different from Report)

Same

18. SUPPLEMENTARY NOTES

RADC Project Engineer: John A. Graniero (DCCD)

19. KEY WORDS (Continue on reverse side if necessary and identify by block number)

Adaptive Systems	Adaptive Arrays
Adaptive Filters	Null Steering
Adaptive Antennas	IIR Filters

20. ABSTRACT (Continue on reverse side if necessary and identify by block number)

Conventional adaptive array processing is accomplished by linearly combining the outputs of tap delay lines attached to each sensor of an array. This type of processing can be interpreted as using an "all-zero" filter at each sensor to generate a frequency-dependent magnitude and phase shift (weighting) over the operating bandwidth of the array.

A new array processing method is presented which uses filters possessing both poles and zeros to perform the frequency-dependent weighting. (over)

DD FORM 1 JAN 73 1473 EDITION OF 1 NOV 65 IS OBSOLETE

UNCLASSIFIED

SECURITY CLASSIFICATION OF THIS PAGE (When Data Entered)

Adaptation of these filters is based on minimization of the "equation error" rather than the true output error. Ramifications of the equation error approach to array processing are discussed. The idea of constrained array processing is discussed and an optimal array weighting formula is derived. The effects of thermal noise on optimal array weighting and pole and zero filtering is presented. Through computer simulations, the pole and zero method is shown to substantially improve the wideband interference nulling capabilities of the array, providing sharper and deeper nulls while using the same total number of weights as an "all zero" filter. The method is expected to be useful in many seismic, acoustic, and electromagnetic array processing applications.

TABLE OF CONTENTS

A

I. INTRODUCTION

The field of adaptive array processing has been in existence for the past two decades. Foundations of the field were laid by Howells and Applebaum with the introduction of the adaptive sidelobe canceller in 1965-1966 [1,2] and by Widrow et. al. with the development of the broadband adaptive antenna in 1967 [3]. Also in 1967 and the year following, Capon et. al. and Lacoss published articles detailing their work on the signal processing of data from a large aperture seismic array [4,5]. Since then, a variety of different adaptive array processing techniques have been described in the literature [5-15]. During that period, a type of processing called constrained array processing was developed [4,6,7,10,14]. One of the more notable papers on this subject is the one by Frost [7].

In this paper, we introduce a new linearly constrained adaptive array processing technique which performs the frequency-dependent array weighting using filters possessing both poles and zeros. It is shown that the need for such weighting arises when the relative bandwidth of the received signals is large.

In section II, we begin by deriving the optimal array weighting required to eliminate $m-1$ interference sources incident on an m-element array with a constrained look direction. The form of the optimal weighting is later used as motivation for the development of an adaptive array processor based on pole-zero filters. Also in the section, we analyze the effect of isotropic thermal noise on the optimal weighting. Concluding this section is a brief discussion of the relationship between a constrained processor and a Howells-Applebaum processor.

In section III, the issue of approximating the optimal array weighting is addressed. The all-zero and all-pole filter models are presented. Section IV introduces an alternate implementation of a conventional Frost array processor and analyzes its performance as a function of the number of taps. Simulations of the conventional Frost array processor are presented for the purpose of comparing with the pole-zero Frost array processor developed in section V.

In section V, problems associated with the adaptation of pole-zero filters are discussed. It is shown how a simple reformulation of the adaptive filter error function eliminates many of these problems. Two undesirable attributes of the error reformulation are discussed along with ways of overcoming them. Simulations are presented which show that the new pole-zero processor can offer a substantial improvement in the array performance compared to that obtained using the conventional all-zero method.

II. OPTIMAL CONSTRAINED ARRAY PROCESSING

Overview

A constrained array processor such as the one proposed by Frost, operates in an environment where a single desired signal is incident upon an array from a known direction and several interference signals are incident from other unknown directions. The objective of Frost's processor is to minimize the response of the array in the direction of the interference signals while leaving the response in the look direction unaltered or fixed at a specified value. A block diagram of a Frost array with a unity gain look-direction constraint is shown in Figure 1. Throughout this paper Z-transform notation is used to indicate a fixed linear digital filter. Conversion from the Z-domain to a function of frequency is accomplished through the substitution $z=e^{j\omega T}$, where ω is the radian frequency and T is the sampling period. In Fig. 1, the look direction is assumed to be perpendicular to the array axis. A non-perpendicular look-direction can be accommodated by adding alignment filters, usually in the form of steering delays, to each sensor to cause the look-direction signal to appear in time coincidence at the output of each delay. Such a system is often referred to as a signal-aligned array [17]. After alignment, each signal is passed through a linear filter which serves as the frequency-dependent array weight. The output of all the filters are summed to form the overall array output. Because the look-direction signal appears identically at the input to each array filter, it will experience a response through the array determined by the sum of all the array filters. This sum is constrained to unity in order to maintain an undistorted response in the look direction. Subject to the unity-sum constraint, the filters are adjusted to minimize the output

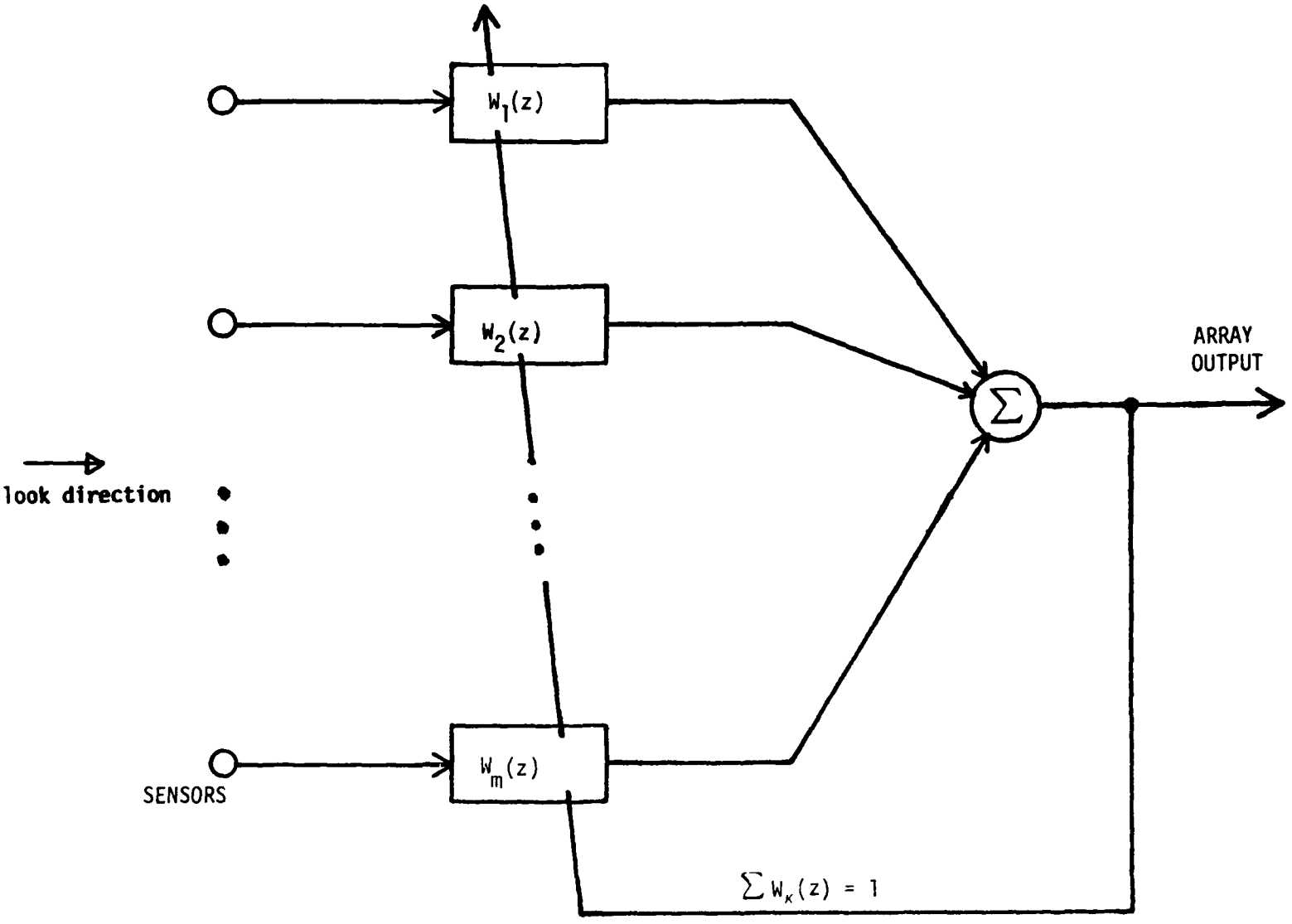

Figure 1. Block diagram of a Frost array with unity gain look-direction constraint.

power of the array and in this manner eliminate interference signals without distorting the look-direction signal.

Optimal array weighting -- Deterministic formulation

We now derive the optimal frequency-dependent array weighting required to cancel $m-1$ broadband directional interference sources incident upon an m-sensor array with a constrained look-direction response. The following analysis assumes ideal propagation conditions and negligible thermal noise.* Let the Z-transform of the look-direction signal be $S(z)$ and the transform of the l^{th} interference signal be $R_l(z)$. Since the look-direction signal appears identically at all sensors of the array, maintaining zero distortion in the look-direction requires that

$$S(z) \sum_{k=1}^{m} W_k(z) = S(z) \quad . \tag{1}$$

Cancelling S(z) from both sides of eq. (1) leaves

$$\sum_{k=1}^{m} W_k(z) = 1 \quad , \tag{2}$$

the look-direction constraint. For simplicity, assume a uniformly-spaced linear array. With such an array, each interference signal undergoes a propagation delay, Δ_l, between adjacent sensors. This delay is determined by the wave propagation velocity c, the sampling rate T, the intersensor spacing d, and the difference in angle between the interference direction and the look direction θ_l,

*In this paper any signal that is uncorrelated from sensor to sensor is referred to as thermal noise.

$$\Delta = \frac{d}{c \cdot T} \cdot \sin\theta_l \quad .$$

Complete cancellation of all interference signals requires that

$$R_l(z) \sum_{k=1}^{m} W_k(z)\, z^{-(k-1)\Delta_l} = 0 \tag{3}$$

for $l=1,2,\cdots,m-1$. Equations (1) and (3) can be written in matrix form as

$$\mathbf{A(z)} \cdot \mathbf{W(z)} = \begin{pmatrix} S(z) \\ 0 \\ \cdot \\ \cdot \\ \cdot \\ 0 \end{pmatrix} \tag{4}$$

where,

$$\mathbf{A}(z) = \begin{pmatrix} S(z) & & & \\ & R_1(z) & & 0 \\ & & \cdot & \\ & & & \cdot \\ & 0 & & \cdot \\ & & & R_{m-1}(z) \end{pmatrix} \cdot \begin{pmatrix} 1 & 1 & \cdots & 1 \\ 1 & z^{-\Delta_1} & \cdots & z^{-(m-1)\Delta_1} \\ \cdot & \cdot & & \cdot \\ \cdot & \cdot & & \cdot \\ \cdot & \cdot & & \cdot \\ 1 & z^{-\Delta_{m-1}} & \cdots & z^{-(m-1)\Delta_{m-1}} \end{pmatrix} \tag{5}$$

and

$$\mathbf{W(z)} = \begin{pmatrix} W_1(z) \\ W_2(z) \\ \cdot \\ \cdot \\ \cdot \\ W_m(z) \end{pmatrix} . \tag{6}$$

By induction, it can be shown that the solution to this set of linear equations is

$$\begin{bmatrix} W_m(z) \\ \cdot \\ \cdot \\ \cdot \\ W_2(z) \\ W_1(z) \end{bmatrix} = \left(\prod_{k=1}^{m-1} \frac{1}{(1 - z^{\Delta_k})} \right) \begin{bmatrix} 1 \\ -\sum \textit{ all single advances} \\ \sum \textit{ all advance pairs} \\ \cdot \\ \cdot \\ (-1)^{m-1} z^{(\Delta_1 + \cdots + \Delta_{m-1})} \end{bmatrix} . \qquad (7)$$

The above frequency-dependent weighting applied to a linear uniformly spaced array would cause all of the interference signals to be perfectly nulled regardless of their bandwidth. Notice that the optimal weighting contains a set of $m-1$ pole-like resonances common to all sensors of the array. This fact will be used later in the paper when developing a pole-zero array processor. Also note that since the intersensor delays can be fractional and the frequency resonances caused by the poles are infinite, an exact rational realization of this weighting is not possible. Instead, one must be content with a rational approximation made over a selected bandwidth. The issue of approximating the optimal weighting will be addressed further in the next section.

To gain insight into the frequency response of the optimal weighting, consider a single inteference source incident on a two-sensor array. In this case, $m=2$ and the optimal weight transfer functions are:

$$W_1(z) = \frac{-z^{-\Delta}}{1 - z^{-\Delta}} \quad \text{and} \quad W_2(z) = \frac{1}{1 - z^{-\Delta}} . \qquad (8)$$

Typical values of Δ fall between $+2$ and -2. Figure 2 shows one period of the frequency response of the optimal weights found by evaluating eqs. (8) with $z=e^{j\omega T}$. Normalized frequency is defined as ωT and ranges between 0 and π/Δ. From these plots it is evident that the magnitude of the optimal weight transfer

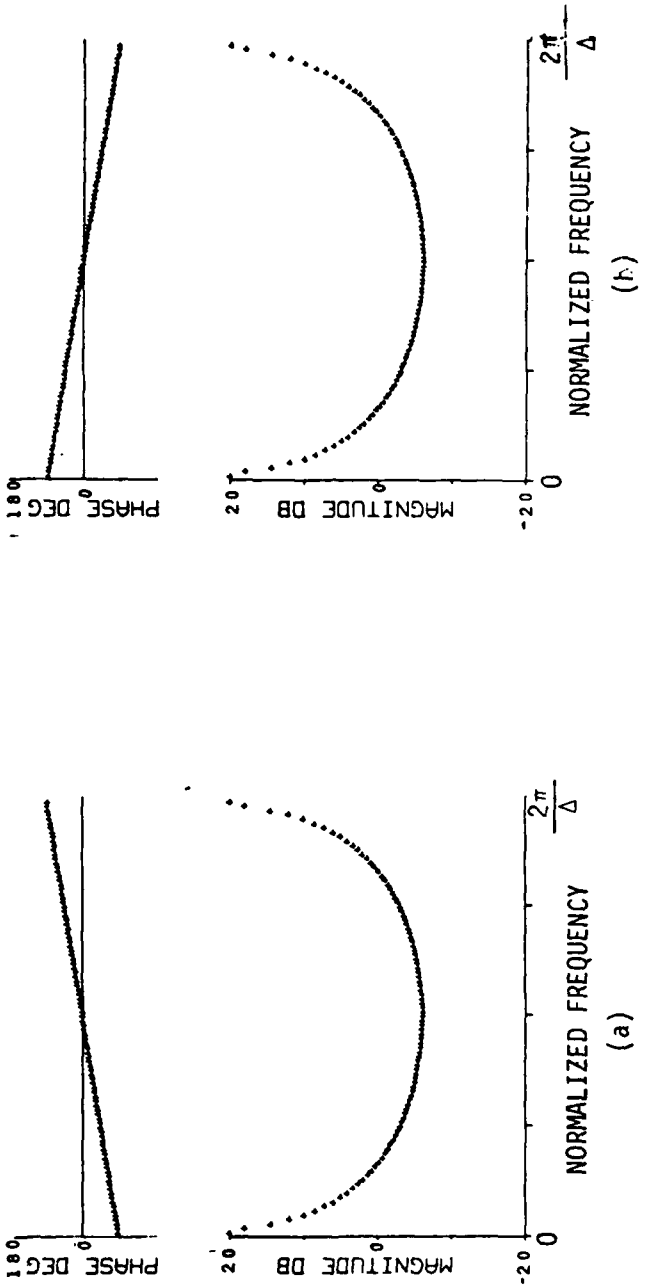

Figure 2. Frequency response of optimal array weights for a two-element Frost array with a single interference source incident on the array. The jammer arrival angle and sampling rate determine the intersensor delay Δ. (a) Sensor 1 (b) Sensor 2.

functions are equal and dependent upon frequency. Also it can be seen that the phase responses are linear and of opposite slopes. The infinite resonance at zero frequency indicates that it is physically impossible to maintain both unity d.c. gain in the look direction and a d.c. null in the interference direction. Notice also that reducing the value of the intersensor delay Δ causes an expansion of the frequency scale of this plot.

Effect of thermal noise on the deterministic solution

When considering the effect of thermal noise on the array output, it turns out that in some situations the weighting given by eq. (7) will perfectly null the directional interference sources but at the expense of exagerating the thermal noise contribution to the array output. Thus, while the signal-to-interference ratio is dramatically improved, there could be a substantial degradation in the signal-to-thermal-noise ratio. Such an effect is easily demonstrated by calculating the thermal noise power at the array output as a function of the intersensor delay Δ. The power spectrum of the array output due to thermal noise is the norm square of the weight vector times the noise power,

$$|Y_n(z)|^2 = \frac{N_o}{2} \cdot |\mathbf{W}(z)|^2 \quad . \tag{9}$$

For the two-sensor case presented above, eq. (9) becomes

$$|Y_n(z)|^2 = \frac{N_o}{(1-z^{-\Delta})(1-z^{\Delta})} \quad . \tag{10}$$

Eq. (10) is plotted in Fig. 3 as a function of the intersensor delay Δ and with $\frac{N_o}{2}$=.001. Notice that as Δ becomes small, the thermal noise contribution to

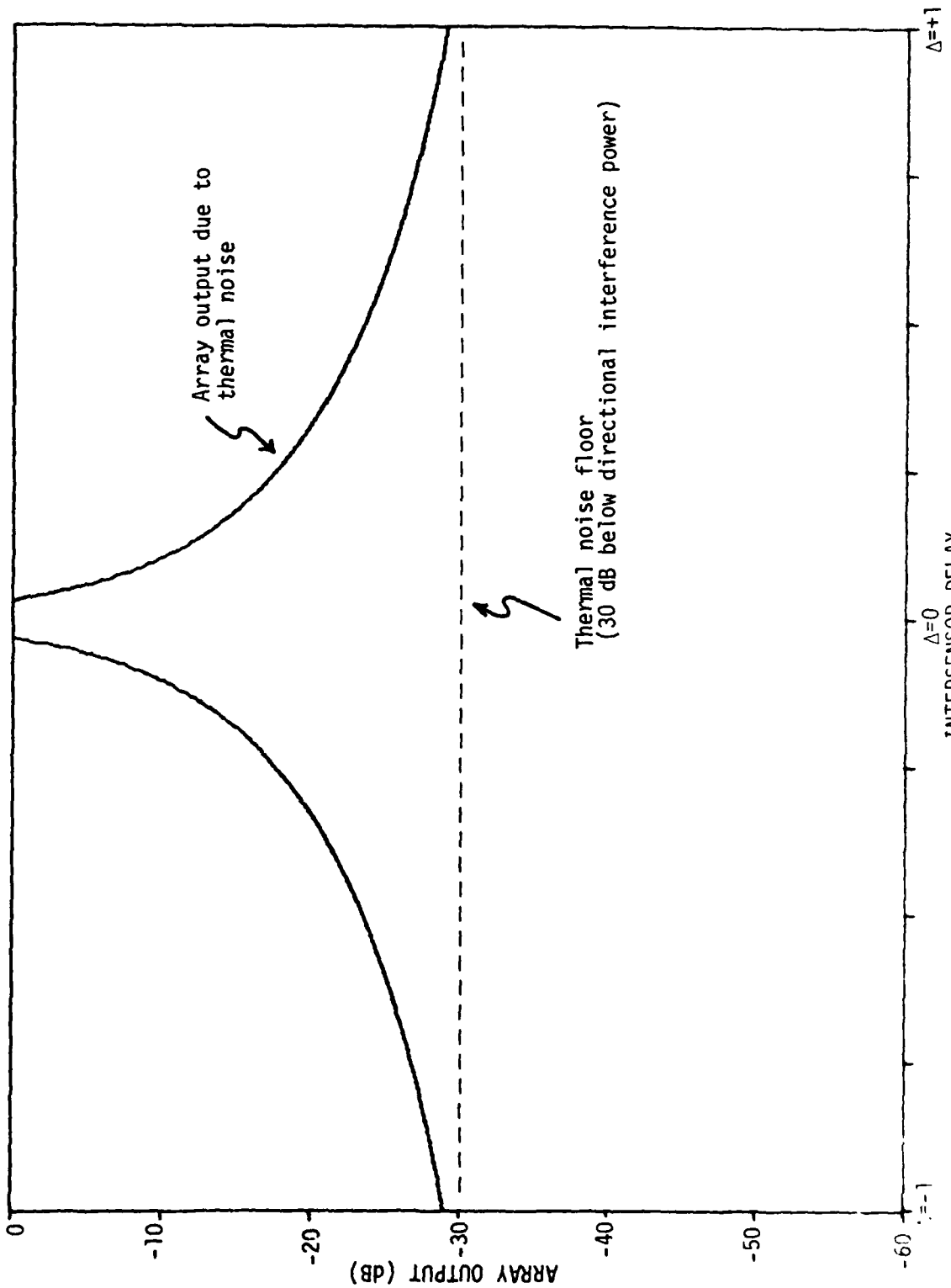

Figure 3. Broadband thermal noise power at array output as a function of intersensor delay. Array weights chosen to completely null directional interference without regard to thermal noise.

the array output becomes large. As Δ becomes large, the thermal noise power appearing at the array output drops to a level equal to the amount of noise added to each sensor (the thermal noise floor). Observation of the converged antenna pattern explains this phenomena. In order to place a null near the look direction, the array antenna pattern billows out in other directions. The increased gain in non-look directions causes the thermal noise at the array output to become large. Thus, when the interference direction is close to the look direction, the effect of a small amount of thermal noise becomes important and must be taken into account.

Optimal array weighting -- Wiener formulation

To overcome the thermal noise problem, a compromise must be made between interference nulling and thermal noise suppression. The Wiener solution accomplishes such a compromise by minimizing the overall array output power subject to a constraint. Using Lagrange multipliers, it can be shown that the frequency-dependent array weights which minimize the mean square of the array output subject to a unity-gain look-direction constraint satisfy the following equations [7]:

$$\mathbf{R}_{ss}(z)\cdot\mathbf{W}(z) = \begin{pmatrix} 1 \\ 1 \\ \cdot \\ \cdot \\ \cdot \\ 1 \end{pmatrix} \Big/ \left\{ 1\ 1\ \ldots\ 1 \right\} \cdot \mathbf{R}_{ss}^{-1} \cdot \begin{pmatrix} 1 \\ 1 \\ \cdot \\ \cdot \\ \cdot \\ 1 \end{pmatrix} , \qquad (11)$$

where $\mathbf{R}_{ss}(z)$ is the mxm spectral covariance matrix of the array signals after alignment and $\mathbf{W}(z)$ is the mx1 vector of optimal frequency-dependent weights.

To connect this set of equations to the deterministic set given in (4), multiply both sides of (4) by $\mathbf{A}^T(z^{-1})$

$$\mathbf{A}^T(z^{-1})\mathbf{A}(z)\cdot\mathbf{W}(z) = \mathbf{A}^T(z^{-1})\cdot\begin{pmatrix} S(z) \\ 0 \\ \cdot \\ \cdot \\ \cdot \\ 0 \end{pmatrix} . \tag{12}$$

Interpreting $|S(z)|^2$ and $|R_l(z)|^2$ as the power spectra of stationary stochastic signals, the matrix $\mathbf{A}^T(z^{-1})\cdot\mathbf{A}(z)$ can be viewed as the spectral covariance matrix associated with the array input vector

$$\mathbf{A}^T(z^{-1})\cdot\mathbf{A}(z) = \mathbf{R}_{zz}(z) . \tag{13}$$

Multiplying out the right hand side of eq. (12) using the definition of $\mathbf{A}(z)$ given in (5), it can be shown that

$$\mathbf{A}^T(z^{-1})\cdot\begin{pmatrix} S(z) \\ 0 \\ \cdot \\ \cdot \\ \cdot \\ 0 \end{pmatrix} = |S(z)|^2\cdot\begin{pmatrix} 1 \\ 1 \\ \cdot \\ \cdot \\ \cdot \\ 1 \end{pmatrix} . \tag{14}$$

It is also easy to see from the definition of $\mathbf{A}(z)$ that

$$[\,1\,0\,\ldots\,0\,]\cdot\mathbf{A}(z) = S(z)\cdot[\,1\,1\,\ldots\,1\,] . \tag{15}$$

Post-multiplying both sides of eq. (15) by $A^{-1}(z)$ then taking the norm square of the result gives

$$[\,1\;1\;\ldots\;1\,]\cdot\mathbf{A}^{-1}(z)\cdot\mathbf{A}^{-T}(z^{-1})\cdot\begin{pmatrix}1\\1\\\cdot\\\cdot\\\cdot\\1\end{pmatrix}=\frac{1}{|S(z)|^2}\quad . \tag{16}$$

Combining eqs. (12,13,14,16) gives

$$\mathbf{R}_{zz}(z)\cdot\mathbf{W}(z)\;=\;\begin{pmatrix}1\\1\\\cdot\\\cdot\\\cdot\\1\end{pmatrix}\Big/\Big(1\;1\;\ldots\;1\Big)\cdot\mathbf{R}_{zz}^{-1}\cdot\begin{pmatrix}1\\1\\\cdot\\\cdot\\\cdot\\1\end{pmatrix}\quad , \tag{11}$$

the Wiener equations. Thus with no thermal noise present, the deterministic formulation given in eq. (4) is equivalent to the Wiener formulation given in eq. (11).

Wiener solution in the presence of thermal noise

Finding a closed form solution to eq. (11) in the presence of thermal noise is a difficult, if not impossible task. To gain insight into the array operation in the presence of noise, an exact solution can be found for a two-sensor array. Let $\frac{N_o}{2}$ be the power of the thermal noise relative to the power of the directional interference. This relative power level could be a function of z (frequency), but for the following analysis it is assumed to be constant. In this case, the solution to eq. (11) is

$$W_1(z) = \frac{-(1+\frac{N_o}{2})z^{-\Delta} + z^{-2\Delta}}{1-(2+N_o)z^{-\Delta}+z^{-2\Delta}} \quad . \tag{17a}$$

and

$$W_2(z) = \frac{1-(1+\frac{N_o}{2})z^{-\Delta}}{1-(2+N_o)z^{-\Delta}+z^{-2\Delta}} \quad . \tag{17b}$$

Note that with thermal noise present, the optimal array weighting is still represented by the ratio of two polynomials as it was in the deterministic case. Also note that when $N_o=0$, pole-zero cancellation occurs and eqs. (17) reduce to eqs. (8).

For the two-sensor case, the contribution of the thermal noise to the array output can be computed using eqs. (9) and (17) and is

$$|Y_n(z)|^2 = N_o \left| \frac{(1+\frac{N_o}{2}) - z^{-\Delta}}{-z^{\Delta}+(2+N_o)-z^{-\Delta}} \right|^2 \quad . \tag{18}$$

The array output due to the directional interference is

$$\begin{aligned} |Y_d(z)|^2 &= |W_1(z)\cdot z^{-\Delta} + W_2(z)|^2 \\ &= (\frac{N_o}{2})^2 \left| \frac{1+z^{-\Delta}}{-z^{\Delta}+(2+N_o)-z^{-\Delta}} \right|^2 \quad . \end{aligned} \tag{19}$$

The array output due to both the direction interference and the thermal noise is found by adding eqs. (18) and (19) to give

$$|Y_{n+d}(z)|^2 = |Y_n(z)|^2 + |Y_d(z)|^2$$

$$= \frac{N_o + (\frac{N_o}{2})^2}{-z^{-\Delta} + (2+N_o) - z^{\Delta}} \quad . \tag{20}$$

To determine the performance of the optimal two-sensor array for a wideband signal, eqs. (18-20) can be integrated over the bandwidth of the signal.

Formulas (18) and (19) were numerically integrated over the frequency range $\pi/4$ to $3\pi/4$ and are plotted in Fig. 4 as a function of the intersensor delay. Compare this graph to the one presented in Fig. 3. Notice that for large Δ, the thermal noise dominates the array output. As Δ becomes small, interference nulling is traded off for thermal noise suppression and the interference signal power dominates the array output. Thus when using the Wiener weighting, directional interference nulling is compromised for the sake of thermal noise suppression.

Relationship between a Frost array and a Howells-Applebaum array

The Howells-Applebaum array processor is different from a linearly constrained processor in that it attempts to maximize the SNR of the received signal. In doing so, it allows the desired signal to undergo some distortion as it passes through the array. In this sense, the Howells-Applebaum processor can be thought of as having a soft constraint in the look direction as opposed to the hard constraint used in a Frost processor.

The converged weight vector of a Howells-Applebaum array satisfies the following equation [11],

$$[\, I + \gamma \mathbf{R}_{zz}(z) \,] \cdot \mathbf{W}(z) = v \tag{25}$$

where v is the quiescent steering vector and γ is a constant determined by the

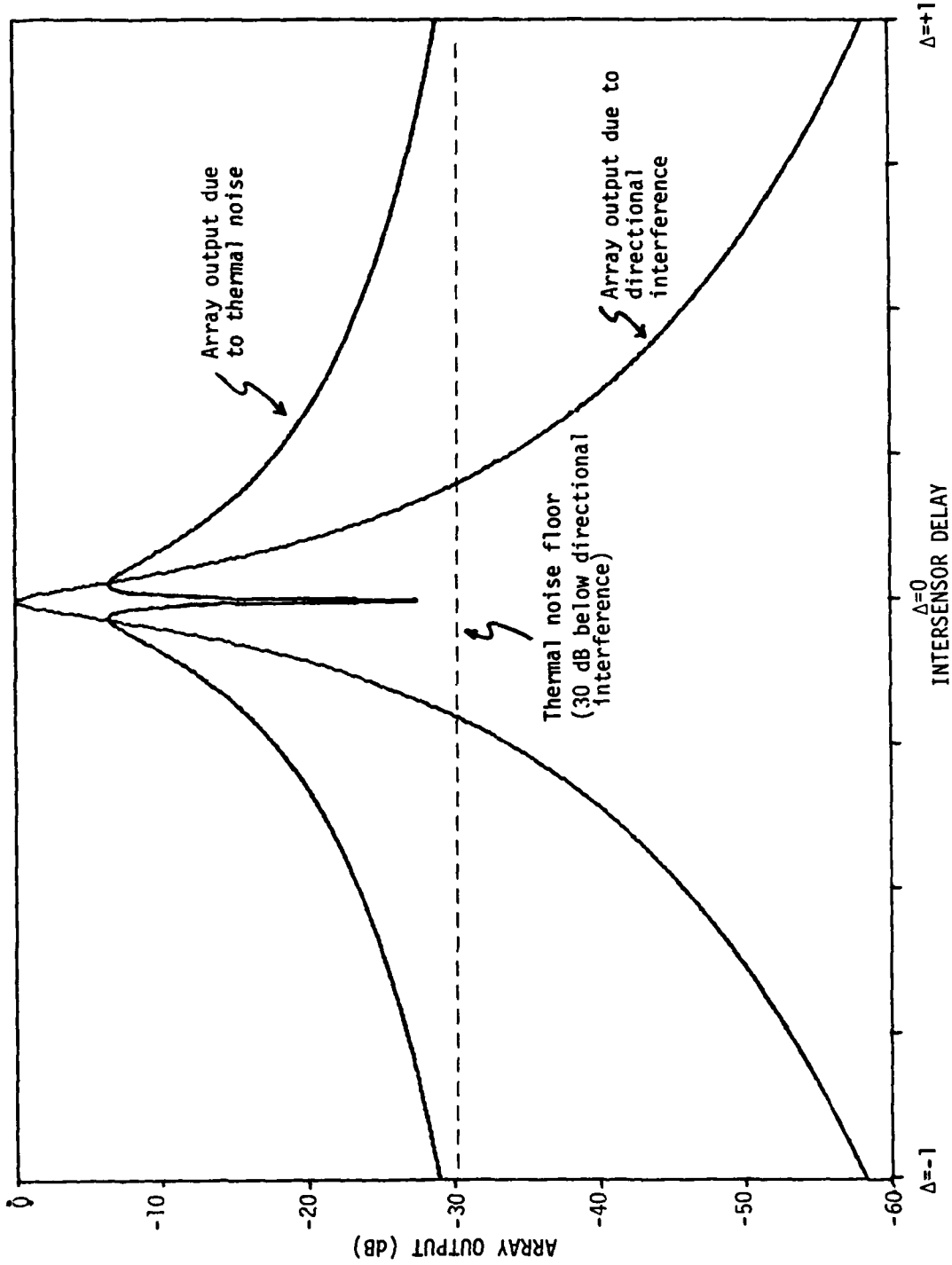

Figure 4. Broadband thermal noise power and interference power at array output as a function of intersensor delay. Array weights chosen to minimize overall array output power subject to look-direction constraint.

dynamic range of the processor. In this paper we have assumed the array to be signal aligned, so,

$$v = \begin{pmatrix} 1 \\ 1 \\ . \\ . \\ . \\ 1 \end{pmatrix} . \tag{26}$$

The solution to eqs. (25) turns out to be similar to the solution expressed by eqs. (11); in the limit as γ goes to infinity, the Howells-Applebaum weight vector and the Frost weight vector differ only by a scalar transfer function. This similarity indicates that a Howells-Applebaum type of array processor could also benefit from the use of pole-zero filters. A soft constrained array processor using pole-zero filters is not investigated in this paper but is left as a topic for future research.

III. APPROXIMATION OF THE OPTIMAL ARRAY WEIGHTING

Role of the relative bandwidth

As was noted in the previous section, the optimal frequency-dependent array weighting is not perfectly realizable. An approximation of the optimal weighting must be made over the array operating bandwidth. An important parameter pertaining to the difficulty of the approximation is the relative bandwidth of the array signals. Relative bandwidth is a dimensionless quantity defined as the ratio between the absolute bandwidth of the received signals and their center frequency. For acoustic, sonar, and seismic arrays, the received signals are at baseband and the relative bandwidth is large. For electromagnetic arrays, the received signals are at radio frequencies and the relative bandwidth is much smaller. In any case, the goal of the adaptive array is to form an approximation of the optimal weighting derived in section II over the operating bandwidth of the array. Simulations depicting the array performance as a function of bandwidth were presented by Rogers and Compton in [18]. Also, an analysis of the nulling performance as a function of bandwidth is given by Mayhan et.al. in [19]. Our paper is concerned not so much with the array performance as a function of bandwidth, but with the improvement of the array performance at a fixed wide bandwidth.

Approximation model

Fig. 5a shows the tap-delay-line filter model commonly used to perform the array weighting in conventional adaptive array processors. It consists of a series of delays whose outputs are linearly combined through the multipliers b_i to form

the filter output. The transfer function of this filter is,

$$H(z) = b_0 + b_1 z^{-1} + \cdots + b_n z^{-n} \quad . \tag{22a}$$

The roots of the H(z) polynomial are called the zeros of the filter.

Fig. 5b shows the direct form realization of an all-pole filter. The filter output is delayed and fed back through the multipliers a_i and summed with the filter input. The transfer function of this filter is,

$$H(z) = \frac{1}{1 + a_1 z^{-1} + \cdots + a_n z^{-n}} \quad . \tag{22b}$$

The roots of the denominator of H(z) are called the filter poles. A cascade of the all-zero and the all-pole filter generates one type of pole-zero filter structure. In this paper, we consider the use of this type of pole-zero filter as the model for approximating the optimal array weighting.

Independence of array weighting on frequency shift

It will now be shown that the difficulty in approximating the optimal array weighting over a specified bandwidth is independent of frequency shift. This implies that down-conversion to an intermediate frequency (IF) or to baseband, will not affect the performance of the array processor.* This is most easily proven by assuming the array signals to be analytic and the array filter coefficients to be complex (as opposed to real). An analytic signal is a complex valued signal whose negative frequency image has been removed by combining the original signal with its Hilbert transform. Recovery of the original signal is accomplished by

*This does not consider hardware implementation issues.

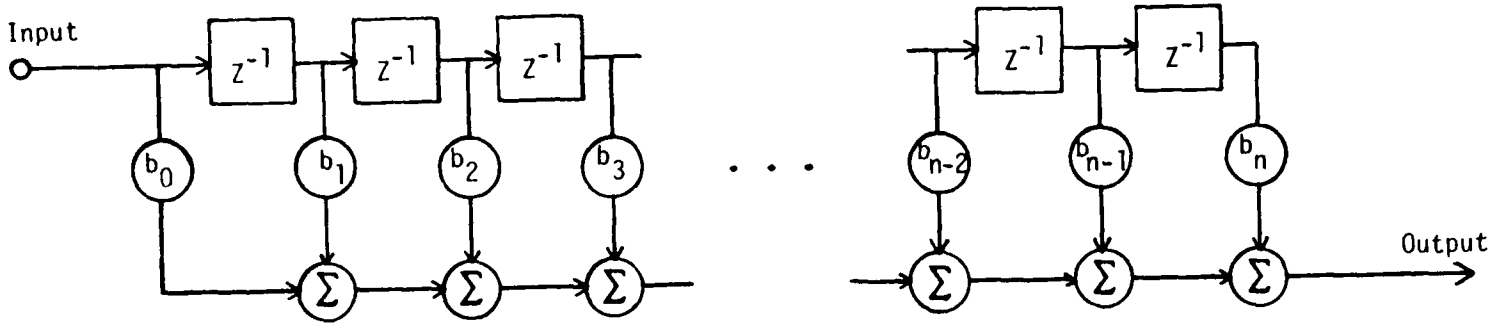

$$H(z) = b_0 + b_1 z^{-1} + \ldots + b_n z^{-n}$$

Fig. 5a. Direct form realization of an all-zero digital filter.

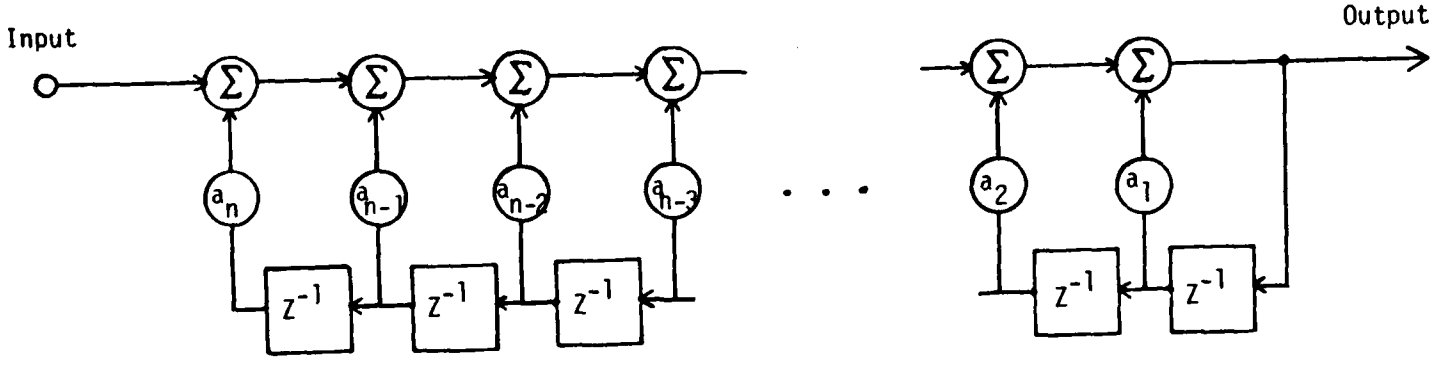

$$H(z) = \frac{1}{1 + a_1 z^{-1} + \ldots + a_n z^{-n}}$$

Fig. 5b. Direct form realization of an all-pole digital filter.

taking the real part of the analytic signal. For more information concerning the analytic representation of array signals, see appendix B of reference [17].

Let the approximation of an optimal array weight be given by

$$\hat{W}(z) = \frac{\sum_{k=0}^{n} b_k z^{-k}}{\sum_{k=0}^{n} a_k z^{-k}} \quad , \tag{23}$$

where $a_0=1$. Note that since the $a_k's$ and $b_k's$ are complex valued, the poles and zeros of this filter do not necessarily occur in complex conjugate pairs. As a function of frequency, eq. (23) can be written as

$$\hat{W}(\omega) = \frac{\sum b_k e^{-j\omega Tk}}{\sum a_k e^{-j\omega Tk}} \quad , \tag{24}$$

where the shifted frequency range is $\omega_1<\omega<\omega_2$. A frequency shifted version of this transfer function is

$$\hat{W}(\omega + \omega_c) = \frac{\sum b_k e^{-j(\omega+\omega_c)Tk}}{\sum a_k e^{-j(\omega+\omega_c)Tk}} \quad , \tag{25}$$

where the pertinent frequency range is $\omega_1-\omega_c<\omega<\omega_2-\omega_c$. Eq. (25) can be easily rewritten as

$$\hat{W}(\omega + \omega_c) = \frac{\sum b_k e^{j\omega_c Tk} e^{-j\omega Tk}}{\sum a_k e^{j\omega_c Tk} e^{-j\omega Tk}} \quad . \tag{26}$$

Letting $\hat{W}'(z)$ be the frequency shifted response, eq. (23) becomes

$$\hat{W}'(z) = \frac{\sum b_k' z^{-k}}{\sum a_k' z^{-k}} \quad , \tag{27}$$

where

$$b_k' = b_k e^{-j\omega_c Tk} \quad \text{and} \quad a_k' = a_k e^{-j\omega_c Tk} \quad . \tag{28}$$

Using the transformation given in eq. (28), we see that $\hat{W}(z)$ and $\hat{W}'(z)$ are equivalent when evaluated over their respective frequency ranges. This proves that approximation of the optimal weighting over a specified bandwidth is independent of frequency shift and implies that an investigation of the bandwidth characteristics of an array need not be concerned with the intermediate frequency of the receiver.

IV. CONVENTIONAL FROST ARRAY PROCESSING

Alternate implementation

To simplify the adaptivity issue, we introduce the alternate constrained array processor shown in Fig. 6. This structure was first discussed by Applebaum and Chapman [13] and more recently shown to be equivalent to a Frost array by Griffiths and Jim [16]. The basic idea of this realization is to use a preprocessor to remove the look-direction signal from the adaptive process x-input making it impossible for the adaptive process to cancel signal components from the array output by subtraction. Interference signals appear in both the x and d inputs and can therefore be cancelled from the output. Such a structure maintains the unity gain look-direction constraint without using a constrained adaptive algorithm. The pole-zero array processor developed in the next section is based on this alternate implementation of Frost's processor. It should be noted that several different types of preprocessors were discussed in [16]. The type shown in Fig. 6 is conceptually the simplest but is not necessarily the best of these.

Transformation between the two array processors is readily seen to be

$$\begin{pmatrix} W_1(z) \\ W_2(z) \\ \cdot \\ \cdot \\ \cdot \\ W_m(z) \end{pmatrix} = \frac{1}{m} \begin{pmatrix} 1 \\ 1 \\ \cdot \\ \cdot \\ \cdot \\ 1 \end{pmatrix} - \begin{pmatrix} 1 & & & \\ -1 & 1 & 0 & \\ & -1 & \cdot & \\ & & \cdot & \cdot \\ & 0 & & \cdot \; 1 \\ & & & -1 \end{pmatrix} \begin{pmatrix} B_1(z) \\ B_2(z) \\ \cdot \\ \cdot \\ \cdot \\ B_{m-1}(z) \end{pmatrix} \tag{29}$$

For the $m=2$ case, this set of equations reduces to

$$W_1(z) = 1/2 - B(z)$$

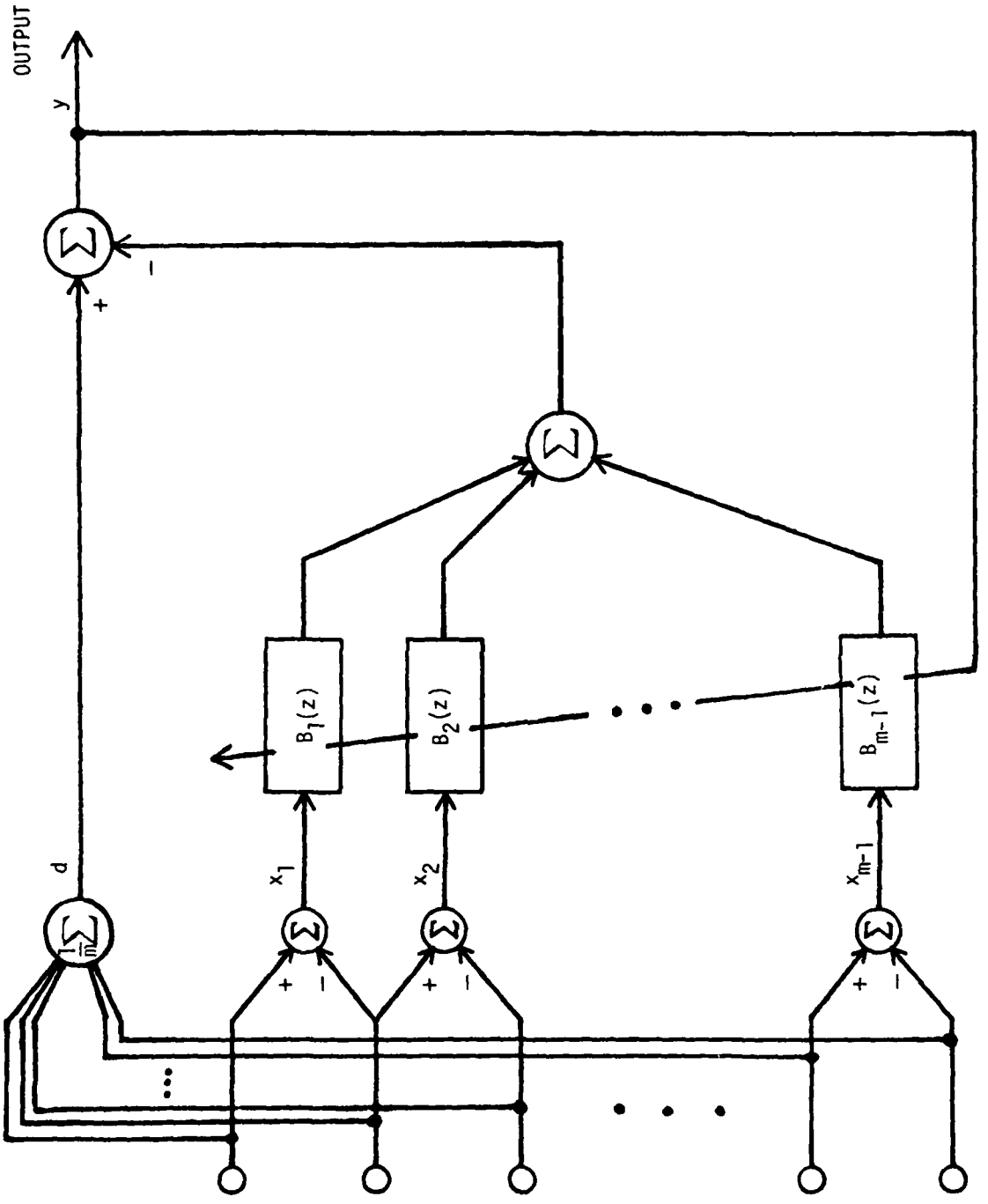

Figure 6. Alternate realization of a Frost array using unconstrained adaptation.

$$W_2(z) = 1/2 + B(z) \quad . \tag{30}$$

Solving eqs. (3) for $B(z)$ gives

$$B(z) = 1/2\,[W_2(z) - W_1(z)] \quad . \tag{31}$$

The optimal transfer function given in eq. (8) thus becomes

$$B(z) = 1/2\frac{1 + z^{-\Delta}}{1 - z^{-\Delta}} \quad . \tag{32}$$

From eqs. (29) and (32) notice that optimal weighting for the alternate Frost array processor still contains a set of poles common to all array weights.

Simulations

We now present simulations of a two-element Frost array processor. In section V of this paper, these simulations will be compared to a similar set of simulations of a pole-zero Frost array processor.

The conditions of the simulation are as follows: The interference signal had a normalized center frequency of $\pi/2$, a 100% relative bandwidth, and a bearing angle 45 degrees off the look direction. There was no thermal noise. The array consisted of two elements spaced one quarter wavelength apart at the signal's center frequency. Such a configuration corresponds to an intersensor delay equal to $\sqrt{2}/2$. The array filters each had 5 taps (4 zeros) and the tap spacing was 1.

Figure 7 compares the frequency response of the converged Frost array filters with the frequency response of the optimal array weighting. The cross-hatched dark lines indicate the optimal frequency response plotted over the bandwidth of the interference. The continuous curve represents the frequency

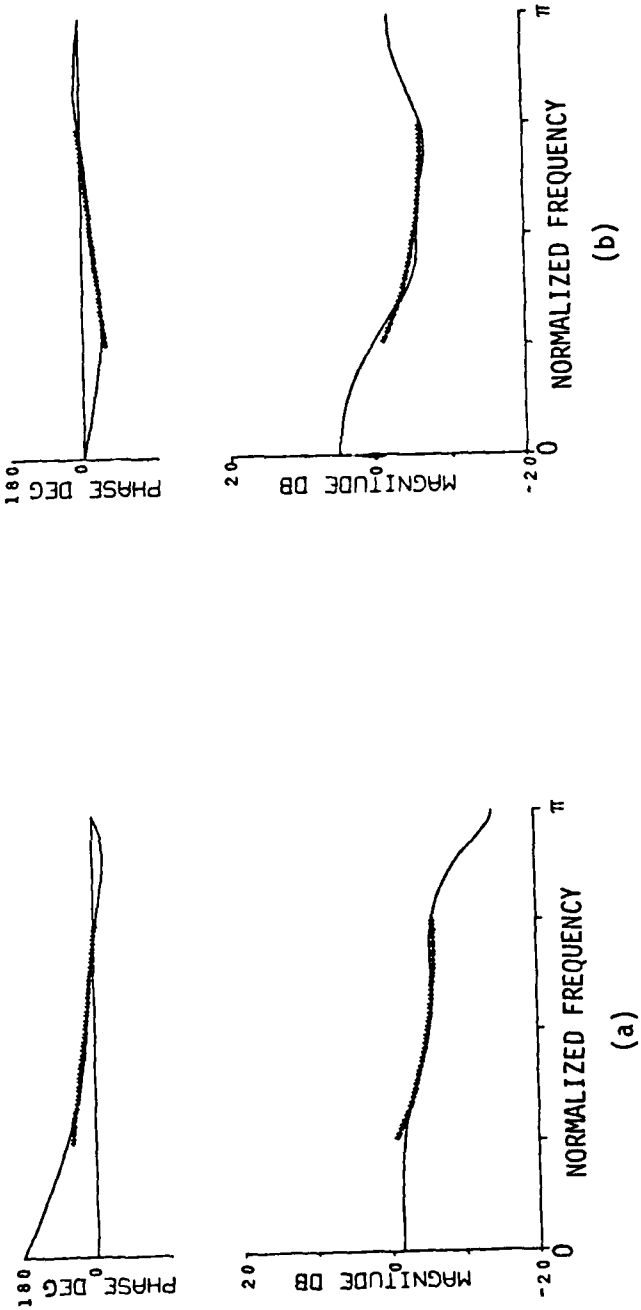

Figure 7. Frequency response of optimal array weights (cross-hatched marks) compared to 5 weight approximation from a Frost array. (a) Sensor 1 (b) Sensor 2.

response of the 4-zero Frost array filter. It is interesting to note that if the relative bandwidth were small enough, the optimal frequency response would need be matched in magnitude and phase at only a single frequency. Such a response could be realized using one complex weight as is the case in most narrowband adaptive array systems. In this paper, however, we are concerned with performance over a wide bandwidth which requires the use of a digital filter, not a single complex weight to perform the array weighting.

Figure 8(a) shows the broadband antenna pattern formed by averaging the array sensitivity over the frequency range of the interference signal. Figure 8(b) shows the frequency response of the array in the look direction. Because the look-direction constraint was set to unity, this response is flat over all frequencies. Figure 8(c) shows the response in the direction of the interference signal. At certain frequencies, the attenuation is as much as 50 dB, but when averaged over the entire interference signal bandwidth, the attenuation is only 20 dB. This simulation thus shows that the Frost array is working fairly well. In section V, we will show that this performance can be dramatically improved using a pole-zero version of Frost's processor.

Figure 9 shows the nulling capability of the Frost array processor as a function of the intersensor delay or equivalently the interference bearing angle. The purpose of this experiment is to show the array performance in the presence of thermal noise and for different interference bearing angles. The condition of this simulation were the same as those in the previous experiment, only -30dB of thermal noise was added The interference bearing angle was scanned from -90°

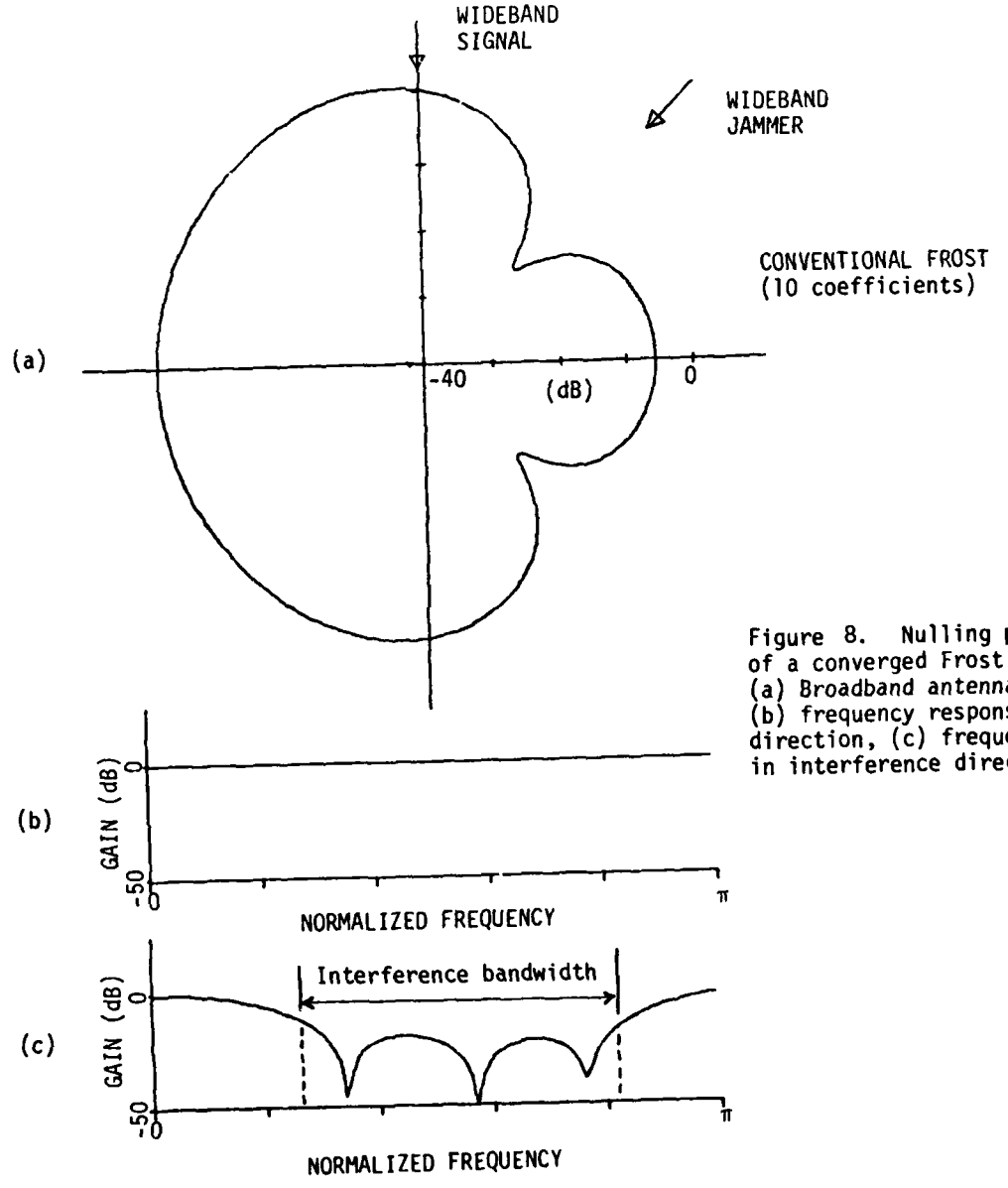

Figure 8. Nulling performance of a converged Frost array. (a) Broadband antenna pattern, (b) frequency response in signal direction, (c) frequency response in interference direction.

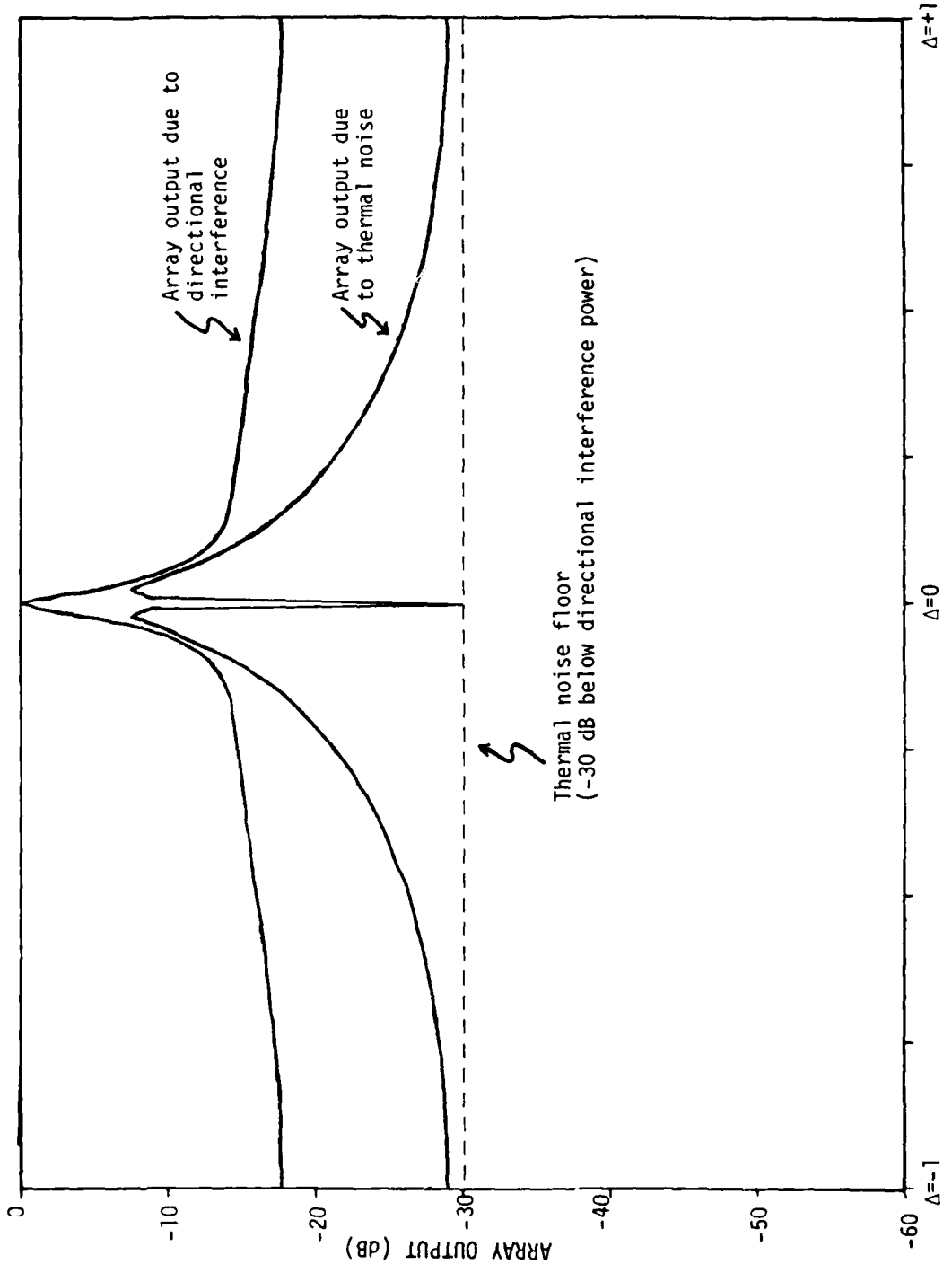

Figure 9. Broadband thermal noise power and interference power at output of a two-element Frost array plotted as a function of intersensor delay.

to $+90^{o}$ corresponding to an intersensor delay ranging between -1 and +1. At each angle, the array was allowed to converge and that the individual contribution to the array output due to thermal noise and to the directional interference was evaluated. Notice that the directional interference dominates the array output for all angles unlike the performance of the optimal array shown in Fig. 4. This occurs because there are not enough weights in the Frost array filters to perform the proper array weighting over the entire interference signal bandwidth. Again this simulation will be compared in section V to a similar simulation of a similar simulation of a pole-zero Frost array processor.

Performance as a function of the number of taps

Intuitively, it is apparent that as more weights are added to the array filters, approximation of the optimal weight frequency response will become more accurate and the null depths will become deeper. It is instructive to determine the performance of a Frost array as a function of the number of taps. An expression for the interference null depth for an arbitrary number of taps can be derived when the interference source is white and incident on the array from an angle corresponding to an intersensor delay of one. In the configuration of the previous experiment, this occurs when the bearing angle is 90 degrees off broadside.

An exact expression for the null depth is found by solving the Wiener equations for an arbitrary dimension. The Wiener solution of the array shown in Fig. 6 is equivalent to the Wiener solution of a Frost array [16] but is somewhat easier to evaluate. Determination of the Wiener equations for the equivalent Frost array proceeds as follows: Since the intersensor delay is one, the Z-transform of

the signal at point x in Fig. 6 is

$$\begin{aligned} X(z) &= R(z) - z^{-1}R(z) \\ &= R(z)\,[\,1 - z^{-1}\,] \quad , \end{aligned} \tag{33}$$

where $R(z)$ is the transform of the interference. The power spectrum of this signal is

$$|X(z)|^2 = |R(z)|^2\,[\,-z^{+1} + 2 - z^{-1}\,] \quad . \tag{34}$$

Interpreting $|X(z)|^2$ and $|R(z)|^2$ as power spectra of stationary stochastic signals and assuming a white interference source, eq. (34) becomes,

$$|X(z)|^2 = -z^{+1} + 2 - z^{-1} \quad . \tag{35}$$

The *nxn* covariance matrix of a signal with a power spectrum given in eq. (35) is a tridiagonal matrix of the form

$$\mathbf{R}_{xx} = \begin{pmatrix} 2 & -1 & & & \\ -1 & 2 & . & 0 & \\ & & . & . & \\ & & . & . & . \\ & 0 & & . & -1 \\ & & & -1 & 2 \end{pmatrix} \quad . \tag{36}$$

Similarly, the cross-correlation vector is

$$\mathbf{P} = \begin{pmatrix} 0 \\ 1/2 \\ 0 \\ . \\ . \\ 0 \end{pmatrix} \quad . \tag{37}$$

The Wiener equations are

$$\mathbf{R}_{zz} \cdot \mathbf{B} = \mathbf{P} \quad . \tag{38}$$

The special tridiagonal structure of these equations allows them to be solved for an arbitrary dimension using mathematical induction. The result is

$$\mathbf{B} = \frac{1}{n+1} \begin{pmatrix} 1/2\,(n-1) \\ n-1 \\ n-2 \\ \cdot \\ \cdot \\ 1 \end{pmatrix} \quad . \tag{39}$$

Using eq. (29), this array weighting can be converted into the equivalent Frost array weighting;

$$\mathbf{W}_1 = \frac{1}{n+1} \begin{pmatrix} 1 \\ -(n-1) \\ -(n-2) \\ \cdot \\ \cdot \\ -1 \end{pmatrix} \quad \text{and} \quad \mathbf{W}_2 = \frac{1}{n+1} \begin{pmatrix} n \\ n-1 \\ n-2 \\ \cdot \\ \cdot \\ 1 \end{pmatrix} \quad . \tag{40}$$

The array response in the direction of the interference source is

$$Y_d(z) = W_1(z) + z^{-1} W_2(z) \quad . \tag{41}$$

Plugging eqs. (40) into eq. (41) gives

$$Y_d(z) = \frac{1}{n+1}(1 + z^{-1} + \cdots + z^{-n+1}) \quad . \tag{42}$$

The power gain of the array to a white interference source is found by taking the sum of the square of the coefficients of polynomial (42) resulting in

$$|Y_d|^2 = \left(\frac{1}{n+1}\right)^2 \cdot (1+1+1+\cdots+1)$$

$$= \frac{1}{n+1} \quad . \tag{43}$$

Eq. (43) indicates that the array power gain for a white interference source is inversely proportional to the number of taps in the two-element adaptive array. Thus, a large number of weights is required in order for the Frost array to form a deep wideband null.

V. POLE-ZERO FROST ARRAY PROCESSING

Motivation

Aside from adding more taps to the array filters, another way to improve the bandwidth characteristics of the array is to use array filters possessing both poles and zeros. In Fig. 2, we see that the frequency response of the optimal array weighting contains infinite resonances at the frequencies 0 and π/Δ. Such resonances are better approximated with filters having both poles and zeros than with zeros alone. In this section, we introduce an adaptive array processing algorithm which adjusts array filters possessing both poles and zeros.

A pole-zero adaptive filter

Development of an adaptive algorithm to adjust pole-zero filters has been the subject of much research. One of the more popular adaptive pole-zero filtering algorithms to appear in the literature is the one by White [28]. This algorithm uses steepest descent to find a minimum of the mean square of the filter's error function. Another popular algorithm is commonly called recursive maximum liklihood (RML) [23] and uses a Newton-type method to find a minimum of the error function. Neither of these algorithms has been entirely successful when applied to problems involving real data. The reasons for this limited success are manyfold. First and foremost is that the mean square error (MSE) is not a quadratic function of the filter's coefficients. This results in an MSE function which has multiple local optima in addition to a global optimum. Furthermore, the MSE becomes infinite when the filter coefficients are adjusted such that the poles of the filter lie outside the unit circle.

Some insight into the above problems is provided by examining the simple single-pole adaptive filter shown in Fig. 10. Let the inputs X_j and d_j be stationary stochastic signals. The MSE of this system can be found in the following manner: The filter output is,

$$\begin{aligned} y_j &= x_j + a_1 y_{j-1} \\ &= x_j + a_1(x_{j-1} + a_1 y_{j-2}) \\ &= x_j + a_1[x_{j-1} + a_1(x_{x-2} + a_1 y_{j-3})] \\ &= etc. \end{aligned} \tag{44}$$

Accordingly,

$$\begin{aligned} y_j &= x_j + a_1 x_{j-1} + a_1^2 x_{j-2} + \cdots \\ &= \sum_{l=0}^{\infty} a_1^l x_{j-l} \ . \end{aligned} \tag{45}$$

For stability,

$$|a_1| < 1 \ . \tag{46}$$

The error ϵ_j is

$$\epsilon_j = d_j - y_j = d_j - \sum_{l=0}^{\infty} a_1^l x_{j-l} \ . \tag{47}$$

Thus the MSE is given by

$$MSE = E[\epsilon_j^2] = E[d_j^2] - \sum_{l=0}^{\infty} E[a_1^l d_j x_{j-l}] + \sum_{l=0}^{\infty} \sum_{m=0}^{\infty} E[a_1^{l+m} x_{j-l} x_{j-m}] \tag{48}$$

Defining the following auto-correlation and cross-correlation functions,

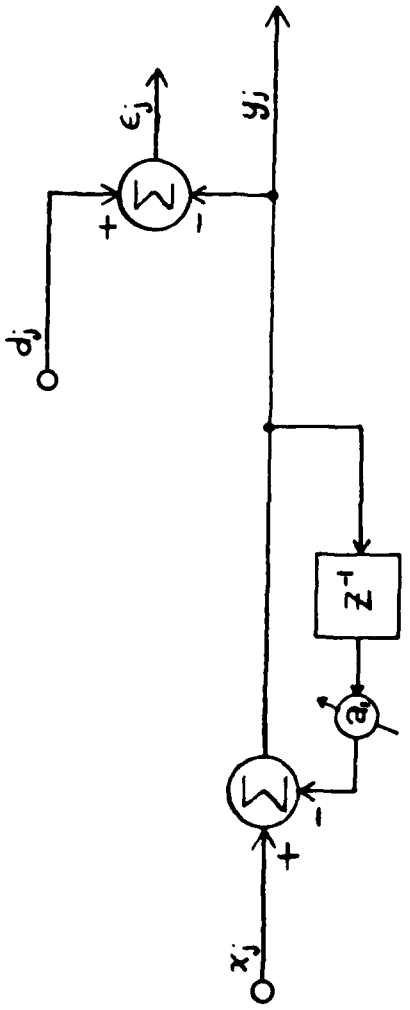

Fig. 10. A single-pole adaptive filter

$$\phi_{xx}(l) = E[x_j x_{j+l}] \tag{49}$$

$$\phi_{xd}(l) = E[x_j d_{j+l}] \ , \tag{50}$$

allows eq. (48) to be written as

$$MSE = E[d_j^2] - 2 \sum_{l=0}^{\infty} a^l \phi_{xd}(l) + \sum_{l=0}^{\infty} \sum_{m=0}^{\infty} a^{l+m} \phi_{xx}(l-m) \ . \tag{51}$$

It is clear from eq. (51) that *the MSE is not a quadratic function of the feedback weight* a_1, but is instead a very complicated function that could have local optima and be very difficult to search. In fact, in an adaptive filter with poles, a general analytical solution for the global minimum does not exist. Also, equation (51) is valid only as long as inequality (46) is satisfied; the MSE goes to infinity when (46) is not satisfied. Such problems do not arise in an all-zero adaptive filter because the mean square error function is a quadratic function of the weights allowing the global solution to be found quite simply by solving a set of linear equations.

Equation-error approach

An adaptive pole-zero array processor could use the RML algorithm to adjust pole-zero filters at each sensor of the array depicted in Fig. 6 in order to minimize the array output. This approach might work for some applications but turns out not to be very robust.

Our approach to adaptive pole-zero filtering bypasses many of the above problems usually associated with pole-zero adaptive filters by reformulating the filter's error function. This is done in a manner which allows the polynomial

associated with the poles of the adaptive filter to be adapted in an all-zero form. The reformulation restores the quadratic nature of the minimization problem to that encountered in the all-zero case and allows easy adaptation using LMS [3], RLS [24], sample matrix inversion [10] or any other least-squares algorithm. A least-squares adaptive lattice implementation of the equation-error array method has been worked out in [25].

Refer to Fig. 11 and assume for the moment that the linear filters are time invariant. The transfer function from point d to the output is unity since the all-pole and all-zero filters cancel.* This cancellation, combined with the fact that the look-direction signal does not appear in the x_k inputs, allows the look-direction signal to pass through the array undistorted. The transfer function from point x_k to the output is $\frac{B_k(z)}{1 + z^{-1}A(z)}$ and contains both poles and zeros. Instead of minimizing the overall array output (which contains the all-pole filter), our approach minimizes the signal appearing at the input to the all-pole filter. In the system identification literature, this signal is often referred to as the equation error [23]. Justification for minimizing the equation error rather than the true output error is that in many cases by making the equation error small, the output error is also made small. Further discussion of the differences between equation error and output error can be found in [27].

The most important aspect of the equation-error approach is that the mean square of the equation error is a quadratic function of the pole polynomial

*Due to their adaptive nature, the array filters are time varying. It is assumed, however, that the adaptation time constant is long compared to the time constant of the filters. In this case, the array filters can be considered time invariant.

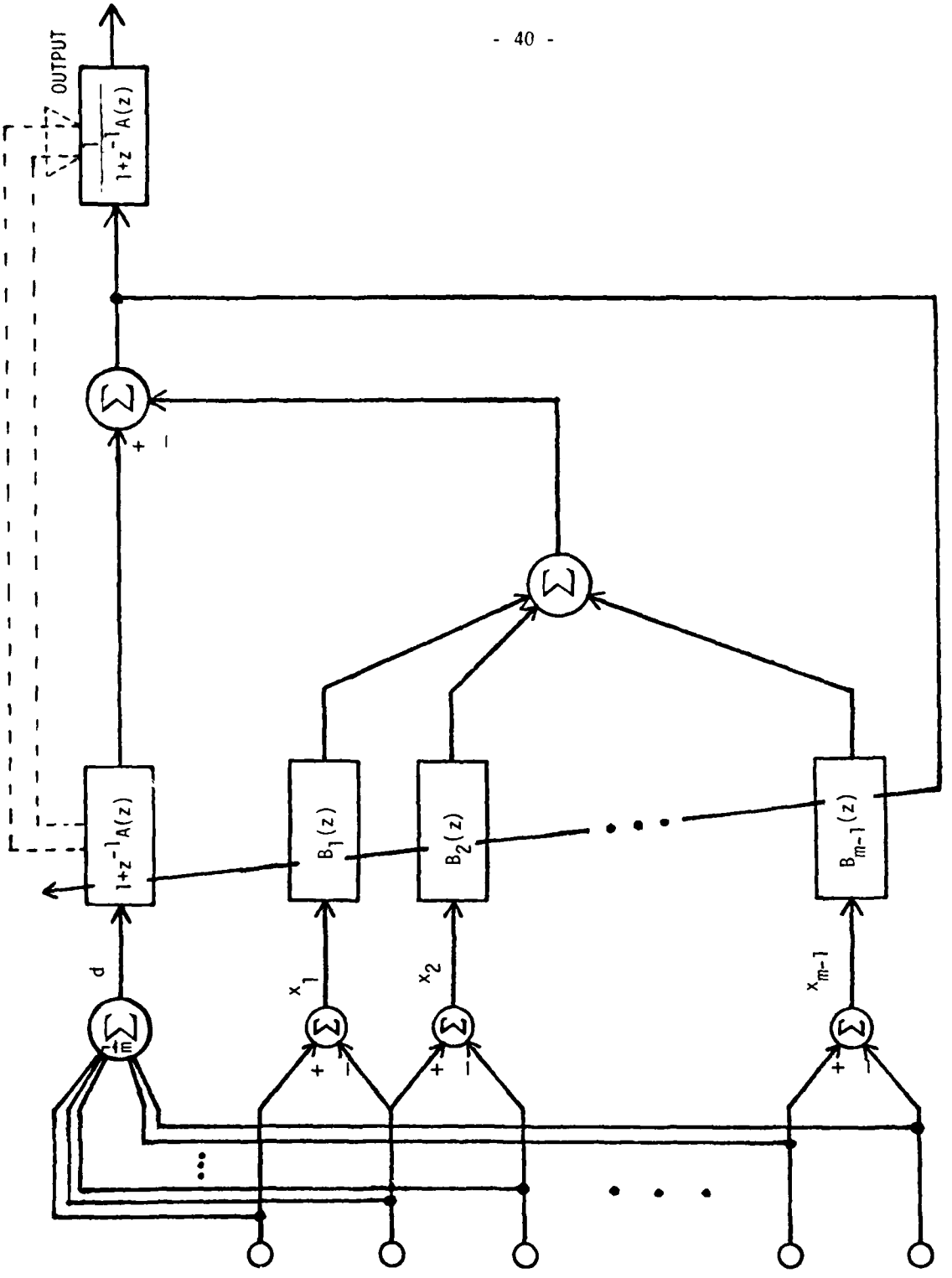

Figure 11. A pole-zero adaptive array processor with unity gain look direction constraint.

coefficients. The convergence rate of the system can be made as fast as the signal-to-noise ratio will allow using sample matrix inversion of other exact-least-squares algorithms. This is not the case in conventional pole-zero adaptive algorithms, such as RML, which minimize the output error. Such algorithms usually exhibit slow convergence and cannot guarantee globality of the converged solution.

To convert the pole-zero array of Fig. 11 into an equivalent array which uses unconstrained adaptation, observe that the transfer function from sensor k to the output is given by

$$W_k(z) = \frac{\frac{1}{m}\,[1+z^{-1}A(z)] - B_k(z) + B_{k+1}(z)}{1+z^{-1}A(z)} \quad , \tag{52}$$

where $B_0(z) = B_m(z) = 0$. It is easily seen that eq. (52) can be equivalently written as

$$W_k(z) = \frac{n_{k0} + z^{-1}N_k'(z)}{1+z^{-1}A(z)} \quad , \tag{53}$$

where $\sum_{k=1}^{m} n_{k0} = 1$ and the $N_k'(z)$ polynomials are unconstrained. This leads to the alternate structural implementation shown in Fig. 12. The similarity between this system and the Frost system shown in Fig. 1 is apparent. Instead of constraining the sum of all the filters to be unity, only the sum of the first coefficients has been constrained. A look-direction signal will experience a transfer function from input to the adaptation error point given by

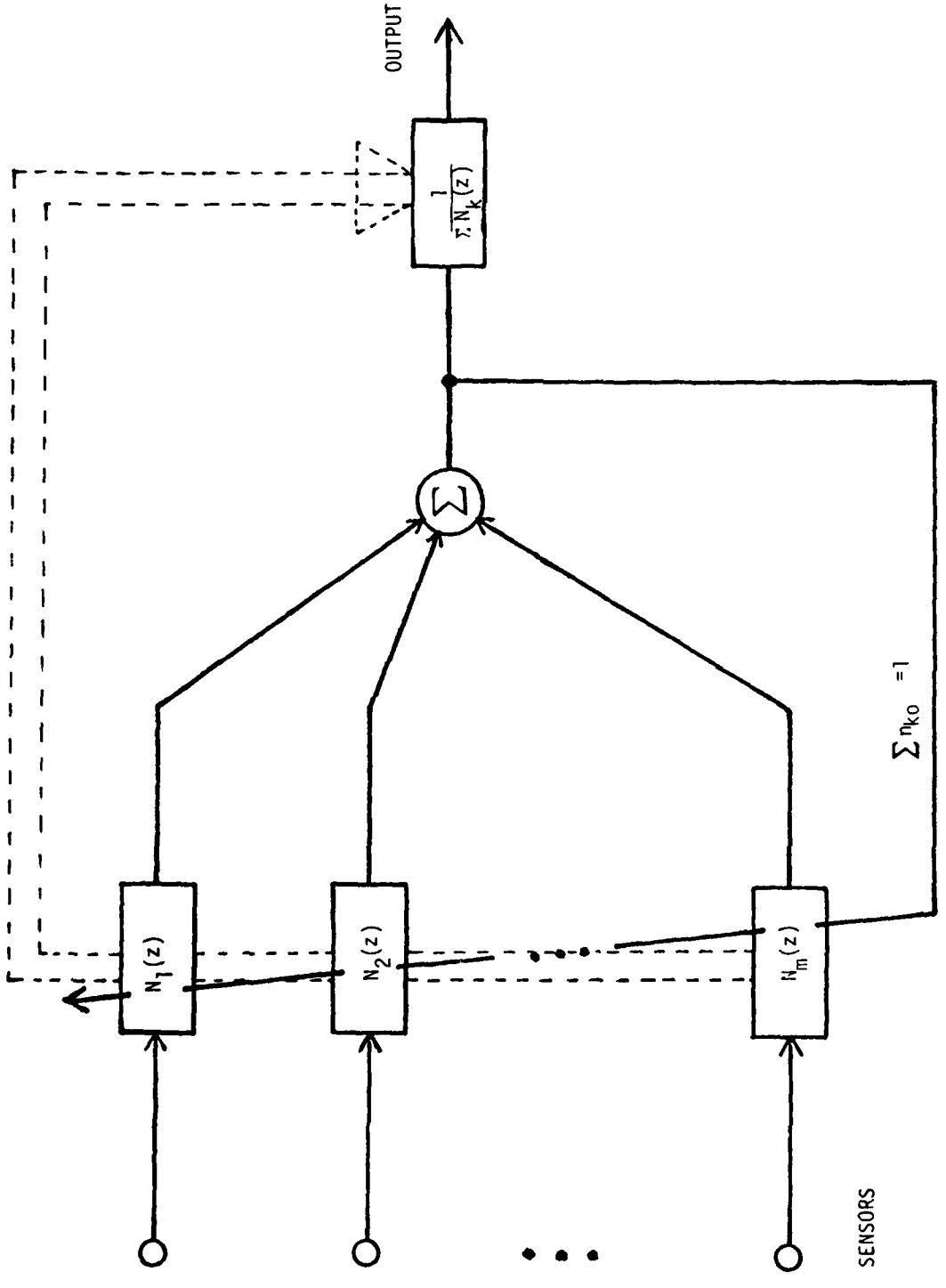

Figure 12. Alternate realization of a pole-zero array processor with unity-gain look-direction constraint.

$$1 + z^{-1} \sum_{k=1}^{m} N_k'(z) \quad . \tag{54}$$

This transfer function is inverted by the all-pole output filter to generate the array output and restore the unity-gain look-direction constraint.

It should also be mentioned that the array processing structure shown in Fig. 12 could be used in non-adaptive applications. For instance, it could be useful in an acoustic application where the objective was to listen in one direction while placing deep wideband nulls in other directions. Knowledge of the directions and spectra of the sources could be used to calculate the coefficients of the array. These coefficients would then be built into a fixed non-adaptive pole-zero array processor.

Stability of the inverse filter

One issue yet to be addressed is that of stability of the inverse filter. In some situations, it is possible that the roots of the polynomial associated with the inverse filter can move outside the unit circle. When this occurs, the inverse filter as shown in Fig. 11 will become unstable and its output will begin to grow without bound.

A pole polynomial with roots both inside and outside the unit circle represents a stable filter only in a noncausal sense. It has an impulse response which is two-sided, extending from $k=-\infty$ to $k=\infty$. Such a response can be approximately realized in a delayed form. For instance, assume that the anti-causal part of the above impulse response extends only to $k=-N$ and is zero from $k=-N$ to $k=-\infty$. By introducing an N-step delay, this impulse response

can be time-shifted so that it is entirely causal and thus realizable. In general, the transfer function can be factored into the product of a purely causal part with all poles inside the unit circle and a purely anticausal part with all poles outside the unit circle. The causal part can be exactly realized. The anticausal part, however, has an impulse response that theoretically extends back to the minus infinity. Practically, the anticausal impulse response has a finite time duration whose length is determined by the proximity of the transfer function poles to the unit circle. The closer the poles are to the unit circle, the longer the impulse response.

One method for overcoming the possible instability of the inverse filter is to approximate it using an all-zero filter. In order to yield an accurate approximation, the all-zero filter needs to be of high order and must be approximated in a delayed form. The consequences of introducing the delay are minimal. The consequences of using a high order all-zero filter as an approximate inverse are a bit more severe. Additional hardware is required to both form and implement the all-zero approximation. At first glance, it might seem as though making a high-order all-zero approximation defeats the original purpose of using poles to economize on weights. However, note that the adaptive algorithm still operates on a reduced number of coefficients. Formation of the approximate inverse can be done off-line and does not introduce complexity into the adaptation. The speed of convergence of the overall system will not be affected. Details of forming an all-zero inverse approximation are given in reference [26].

The preferred method of overcoming the inverse filter instability is to

prevent the pole polynomial roots from ever going outside the unit circle. This can be done in one of two ways. The first way is to constrain the polynomial to remain minimum phase (i.e., keep all roots within the unit circle) during adaptation using a constrained adaptive algorithm which monitors the polynomial roots. The second way is to introduce a bulk delay into the desired response path of Fig. 11. It turns out that increasing the bulk delay causes the roots of the converged pole polynomial to move closer to the origin. Choosing a delay too large causes the resulting solution to lose quality and is not desirable. Choosing a delay too small results in a noncausal solution and an unstable inverse filter. The idea is thus to choose the smallest delay which causes all the roots to lie within the unit circle.

Currently, we are experimenting with several on-line methods for adaptively choosing the above bulk delay. A brute force method is to have a series of almost identical systems all operating on the same input data but each using a different desired response delay. A simple criterion is then used to choose the stable system having the smallest delay. Another method is to use a single system having a variable delay that can be incremented or decremented depending on the stability of the pole polynomial.

Look-direction signal bias

The steady-state Wiener solution of the conventional Frost array is not affected by the presence of a look-direction signal. This is readily apparent by referring to Fig. 6 and noting that the x-input does not contain look-direction signal. Therefore the look-direction signal cannot contribute to either the cross-

correlation between the desired-response input d and the x-input or the auto-correlation of the x-input.

The Wiener solution of the pole-zero Frost array is, however, affected by a look-direction signal. To demonstrate this effect, refer to Fig. 11 and assume that the only source of signal originates from the look direction. In this condition, the x-input will be zero and the d-input will consist of look-direction alone. During adaptation, the $1+ z^{-1}A(z)$ filter will act as a linear predictor and try to reduce the look-direction signal power. If the signal were narrowband, the predictor would in fact form a notch filter at the signal frequency. Distortion of the look-direction signal would not occur since the notch filter response would be inverted by the inverse output filter to restore the look-direction signal at the array output. The main concern is not signal distortion, but the loss of degrees of freedom caused by attempting to internally null the look-direction signal. This degradation is referred to as look-direction signal bias.

In situations where adaptation can be controlled so that it occurs only when the look-direction signal is not present, look-direction signal bias will not occur. This is the case in many radar or spread-spectrum applications where the desired signal is pulsed or sequenced in a manner which is known to the receiver. Also, look-direction signal bias will not cause a significant degradation in the array performance if the look-direction signal power is substantially less than the interference power. In a system where the desired signal is continuous and of significant power, a solution to the bias problem must be found.

One method of alleviating look-direction signal bias is shown in Fig. 13. The

method is based on an idea proposed by Duvall for eliminating dynamic signal cancellation [20,21]. For simplicity, only a three-element example has been shown. The basic idea is to process the set of signals from the sensors in a manner which eliminates the look-direction signal but which keeps the phase relationships among the new set of signals the same as that prior to processing. The processed set of signals is fed into an adaptive "master" array where the Wiener solution cannot be affected by the look-direction signal. The weights of the master array are copied into the "slave" array which operates on the original signal set. Because of the preservation of phase, nulls formed using the slaved array will be in the same directions as those formed in the master. For more details see reference [20].

To analyze the effect of preprocessing on the Wiener solution, we define an effective interference environment that incorporates the preprocessor into the interference sources. Each interference source experiences an angle-dependent frequency transformation when passed through the preprocessor. The frequency response of this transformation is determined by the subtraction of signals appearing at adjacent sensors. Again we assume that the array of sensors is linear and uniformly spaced. A directional interference source will experience a delay, Δ, between two adjacent sensors that is determined by the interference bearing angle. The frequency response of the top subtractor in the preprocessor is given by

$$H(\omega\Delta) = 1 - e^{j\omega\Delta} \quad . \tag{55}$$

Proceeding down the array, each subtractor exhibits this same response plus an

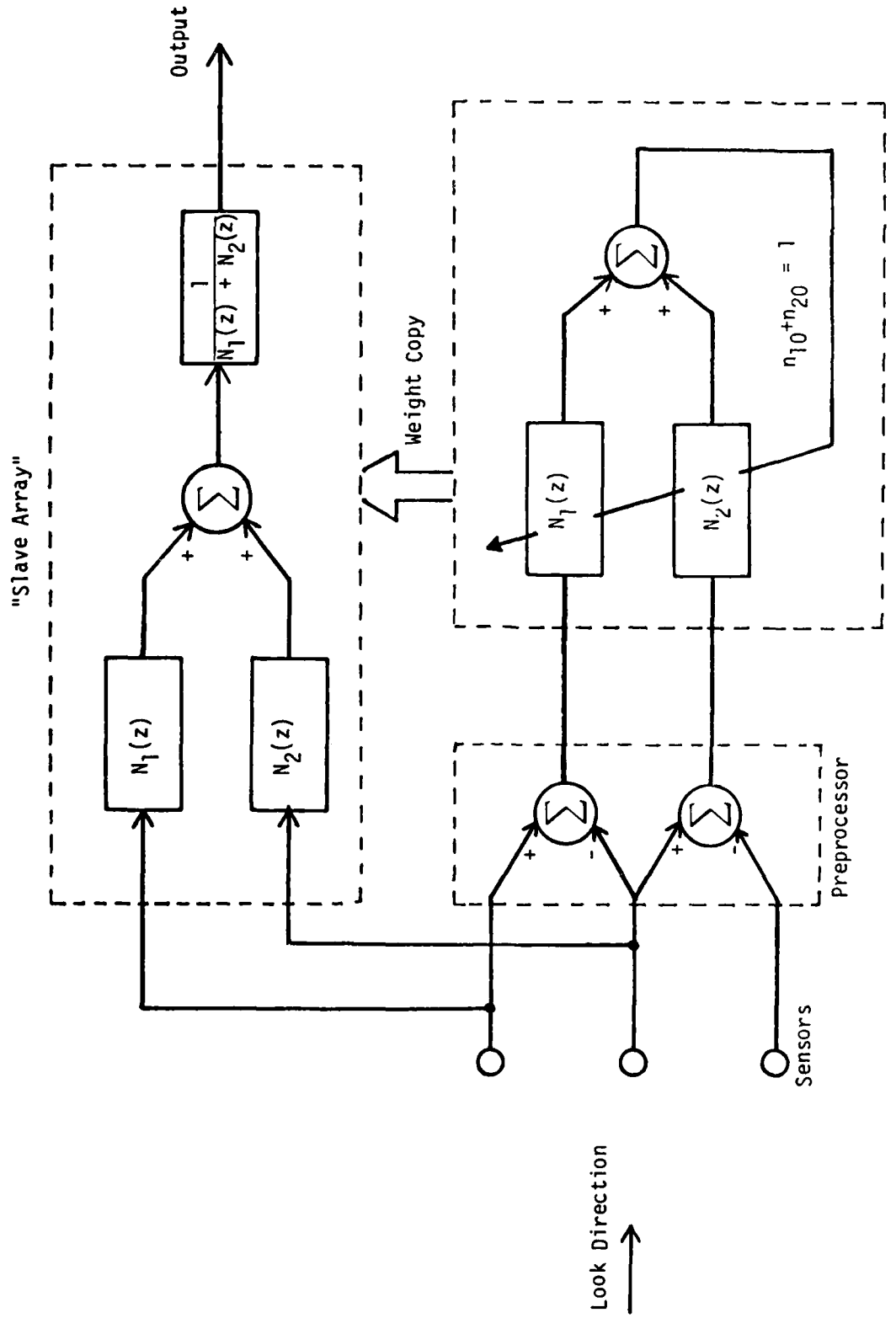

Figure 13. Method for eliminating bias in Wiener solution due to look-direction signal.

additional delay. The idea is to use the $H(\omega)$ transformation to modify the interference source and conceptually eliminate the preprocessor from the array.

Notice that as the interference angle approaches the look direction, the magnitude of the preprocessor transfer function goes to zero. The look-direction signal will be removed and an interference source appearing off the look direction will be somewhat attenuated and high-pass filtered. In this manner, the preprocessor affects the Wiener solution by slightly modifying the weighting applied to the interference source.

Simulations

Figure 14 compares the frequency response of the optimal weight at each sensor with the frequency response of the converged array filters obtained using the proposed pole-zero adaptive array processor. In this simulation, the look-direction signal was assumed to be time-sequenced in a manner which allowed the array to adapt only when the signal was not present. Thus, look-direction signal bias was not a concern. As in the previous simulation, the interference source had a normalized center frequency of $\pi/2$, a 100% relative bandwidth, and a bearing angle 45 degrees off the look direction. Again there was no thermal noise. The array filters had 2 zeros each and 2 common poles. This translates into a total of 8 filter coefficients compared to the 10 coefficients used in the Frost array simulation. Notice that the pole-zero filter response plotted in Fig. 14 is a much closer fit to the optimal response than the conventional all-zero filter response plotted in Fig. 7.

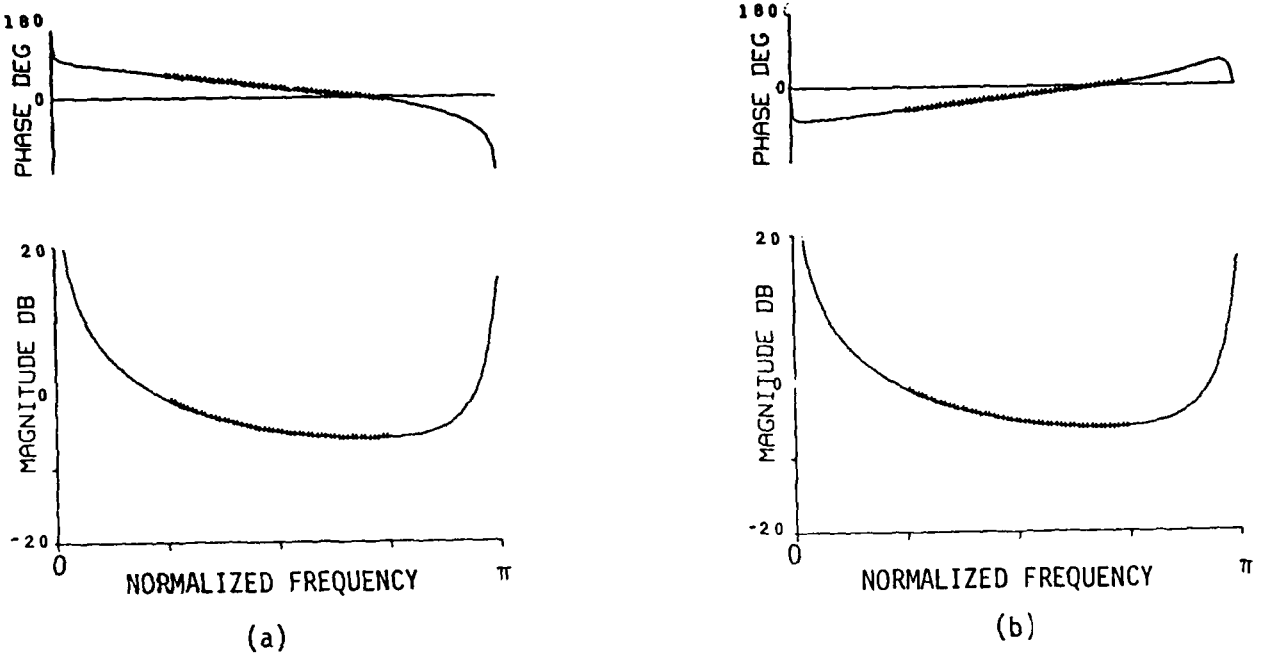

Figure 14. Comparison of frequency response of optimal array weights (cross-hatched marks) with a 2 pole - 2 zero approximation. (a) Sensor 1 (b) Sensor 2.

For further comparison, Fig. 15 shows the broadband antenna pattern and the frequency response of the array in the signal and interference directions. The interference null is about 40 dB below the look-direction gain. *This represents a 20 dB improvement over a conventional Frost system having essentially the same number of variable coefficients.*

Fig. 16 shows the nulling capabilities of a pole-zero Frost array processor as a function of the interference bearing angle. The conditions of this experiment were the same as those given above except that -30 dB of white thermal noise was added to each sensor. Comparing this graph with the one presented in Fig. 9, we see that throughout the field of view, the pole-zero Frost array outperforms the conventional Frost array. Notice that as the interference bearing angle approaches the look direction, the null depth rises to 0 dB and the unity gain look-direction constraint is preserved.

A final set of simulations, shown in Fig. 17, compares the converged broadband antenna pattern of a conventional Frost array with the pattern of a pole-zero Frost array. Both arrays consisted of three colinear uniformly spaced sensors. Incident on both arrays were two mutually uncorrelated wideband interference sources each having a normalized center frequency of $\pi/2$ and a 100% relative bandwidth. The conventional Frost array had 6 zeros per sensor. The pole-zero Frost array had 4 zeros per sensor and 4 poles common to all sensors. Thus, both systems had essentially the same number of variable coefficients. Using an exact least square algorithm, an equal number of coefficients translates into approximately equal convergence rates. Thus the pole-zero Frost antenna pat-

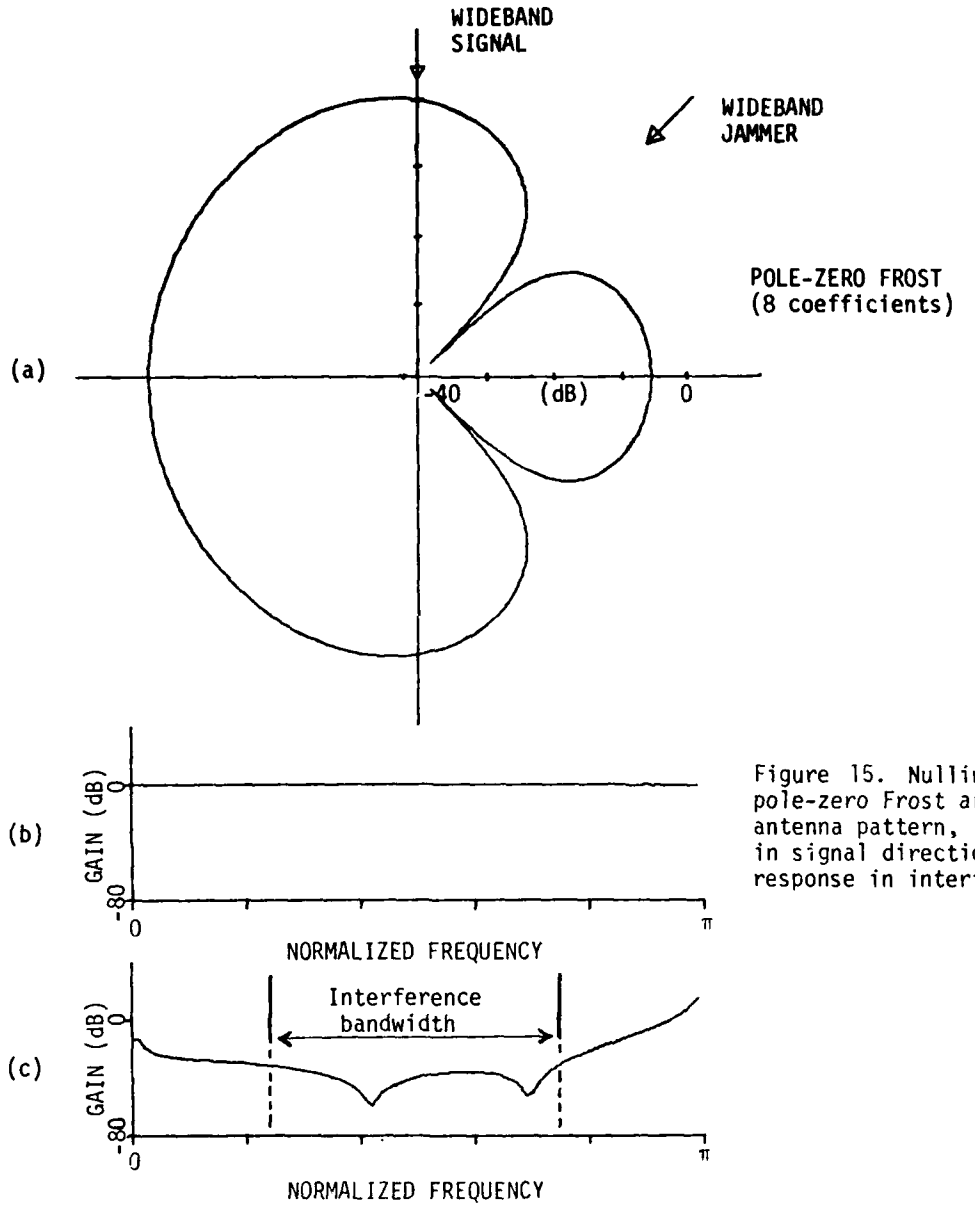

Figure 15. Nulling performance of a pole-zero Frost array. (a) Broadband antenna pattern, (b) frequency response in signal direction, (c) frequency response in interference direction.

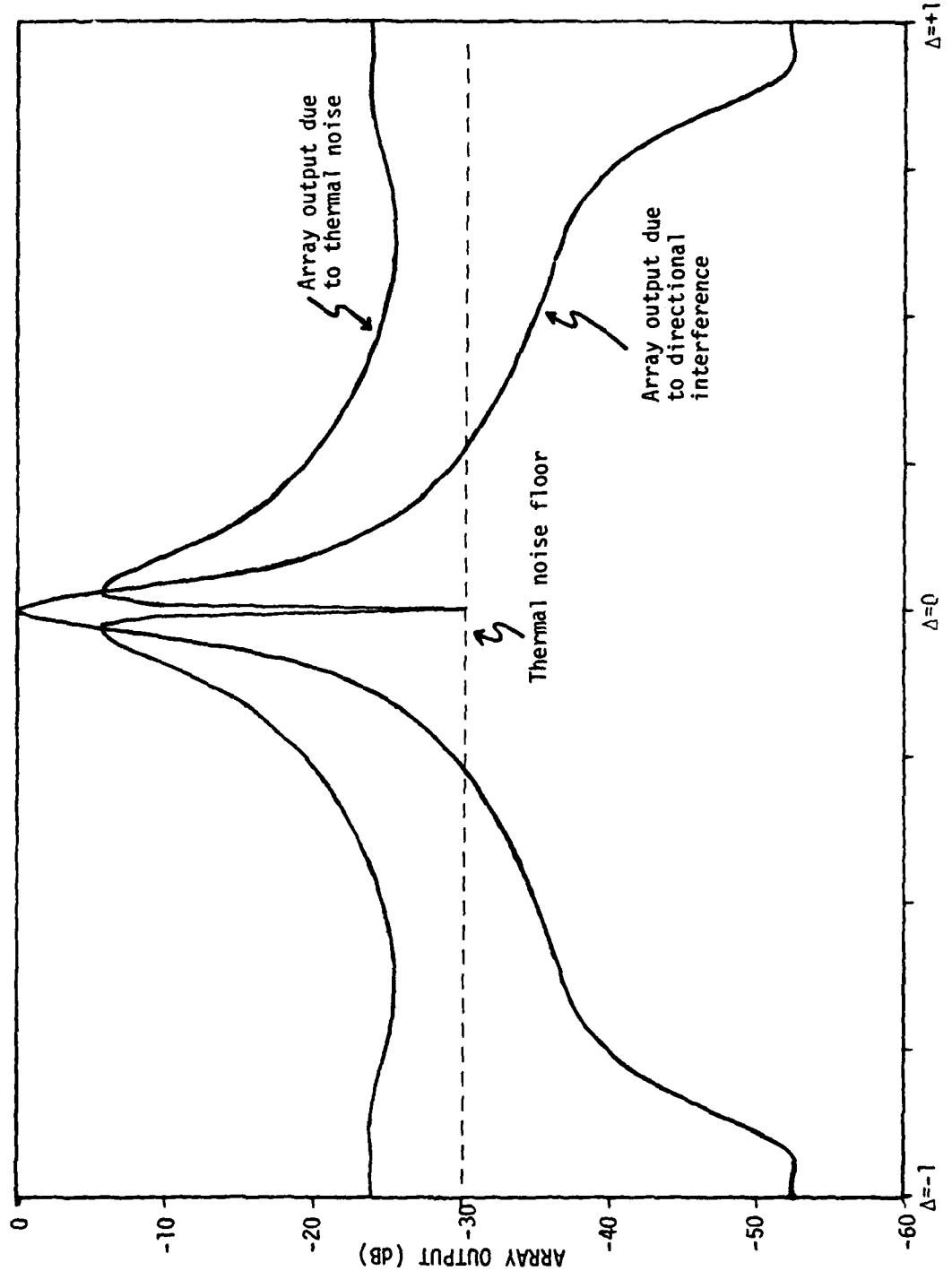

Figure 16. Broadband thermal noise power and directional interference power at output of a two-element pole-zero Frost array plotted as a function of intersensor delay.

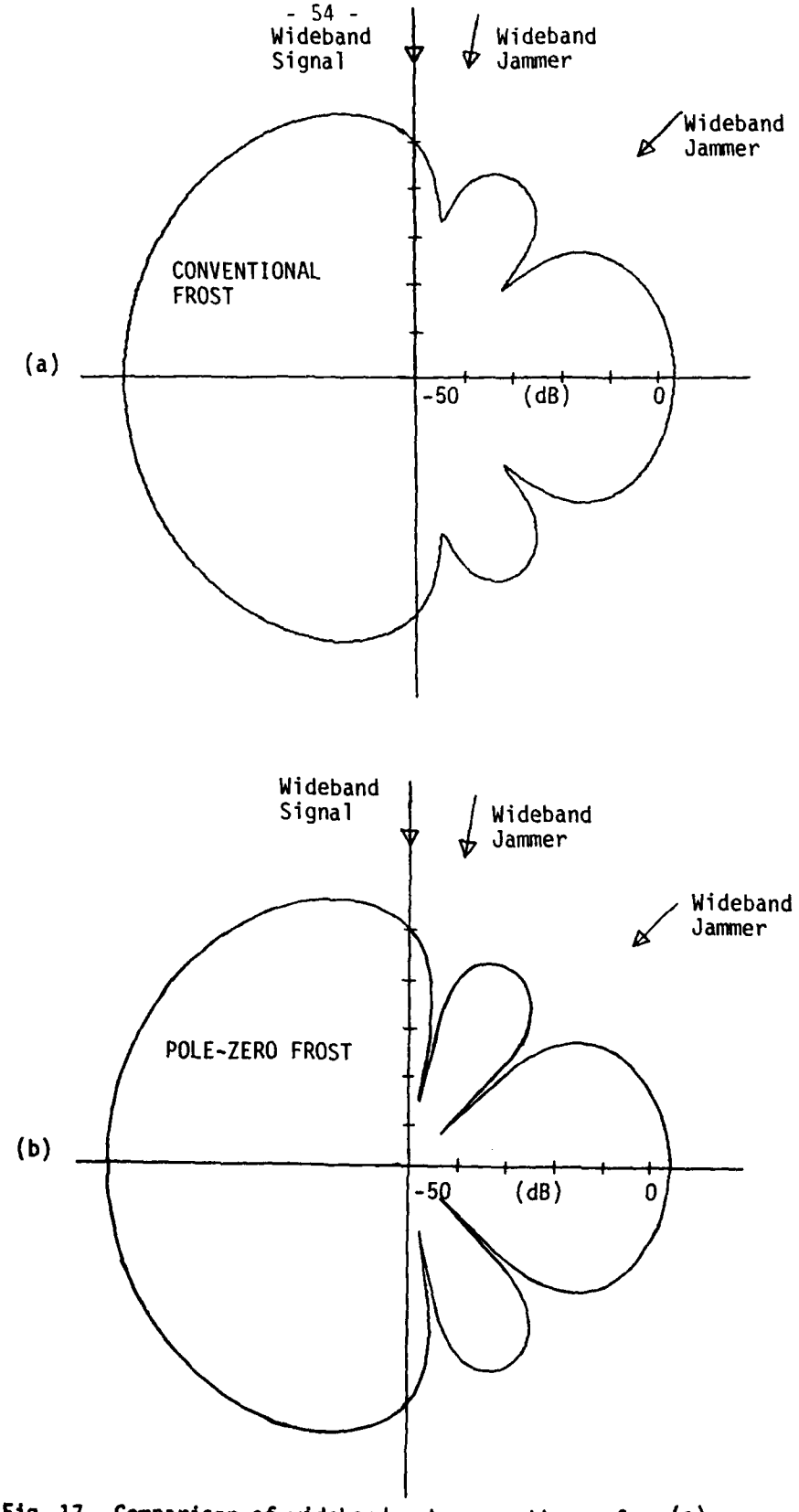

Fig. 17. Comparison of wideband antenna patterns for (a) conventional Frost and (b) pole-zero Frost. Both systems had essentially the same number of weights and convergence rates.

tern shown in Fig. 17b required the same amount of data to reach convergence as did the conventional Frost pattern shown in Fig. 17a.

VI. FUTURE RESEARCH

The work presented in this paper has demonstrated the remarkable utility of the proposed pole-zero adaptive array processor. As with any important new research result, this paper has opened up a wide area for future research. Listed below are a few topics in need of further study.

The application of the pole-zero adaptive processor to nonconformal arrays should be analyzed and simulated. More work should also be conducted concerning stabilization of a nonminimum-phase pole polynomial. The covariance matrix eigenvalue spread should be analyzed in order to determine convergence properties of the pole-zero adaptive array when implemented using the LMS algorithm. Also, the possibility of improved convergence when implementing the pole-zero processor with an adaptive lattice structure should be explored.

VII. CONCLUSIONS

In this paper, a new wideband adaptive array processing structure was presented. Using a derivation of the optimal wideband array weighting function, it was conjectured that filters possessing both poles and zeros would be capable of improving the performance of the nulling array. The "equation-error" approach was developed and used as a method for adapting the poles and zeros of the array filters. The causes and cures of two undesirable attributes of the equation-error approach were discussed. Simulations like the one presented in Fig. 17 demonstrate that the new pole-zero array processor can dramatically improve the wideband nulling capability of the array, providing sharper and deeper nulls while using the same total number of weights.

VIII. REFERENCES

[1] Howells, "Intermediate frequency sidelobe canceller," U.S. Patent 3200390, Aug. 24, 1965.

[2] Applebaum, "Adaptive arrays," Syracuse Univ. Res. Corp., Rep. SPL TR 66-1, Aug. 1966.

[3] Widrow et. al., "Adaptive antenna systems," Proc. IEEE, vol. 55, pp. 2143-2159, Dec. 1967.

[4] Capon et. al., "Multi-dimensional Maximum Liklihood processing of a large aperture seismic array," Proc. IEEE, pp. 192-211, Feb. 1967.

[5] Lacoss, "Adaptive combining of wideband array data for optimal reception," IEEE Trans. Geosci. Electron., vol. GE-6, pp. 78-86, May 1968.

[6] Griffiths, "A simple adaptive algorithm for real-time processing in antenna arrays," Proc. IEEE, vol. 57, pp. 1696-1704, Oct. 1969.

[7] O. L. Frost, III, "An algorithm for linearly constrained adaptive array processing," Proceedings of the IEEE, Vol. 60, No. 8, pp 926-935, Aug. 1972.

[8] N. L. Owsley, "A recent trend in adaptive spatial processing for sensor arrays: constrained adaptation," Signal Processing, Academic Press, pp. 591-604, 1973.

[9] C. L. Zahm, "Applications of adaptive arrays to suppress strong jammers in the presence of weak signals," IEEE Trans. Aerosp. Electron. Sys., AES-9 pp. 260-271, March 1973.

[10] Reed, Mallet, and Brennan, "Rapid convergence rate in adaptive arrays," IEEE Trans. Aerosp. Electron. Sys., AES-10, pp. 853-863, Nov. 1974.

[11] Gabriel, "Adaptive arrays - an introduction," Proc. IEEE, Vol. 64, No. 2, pp. 239-272, Feb. 1976.

[12] Special issue of adaptive antennas, IEEE Trans. Ant. Propogat. vol. AP-24, no. 5, Sept. 1976.

[13] S. Applebaum and D. Chapman, "Adaptive arrays with main beam constraints," IEEE Transactions on Antennas and Propagation, Vol. AP-24, No. 5, pp. 650-662, Sept. 1976.

[14] W. White, "Adaptive cascade networks for deep nulling," IEEE Trans. Ant. Propagat., vol. AP-26, no. 3, pp. 396-402, May 1978.

[15] Horrowitz and Senne, "Performance advantage of complex LMS for controlling narrow-band adaptive arrays," IEEE Trans. on Cir. Sys., vol CAS-28, no. 6, pp. 562-576, June 1981.

[16] L. J. Griffiths, C. W. Jim, "An alternative approach to linearly constrained adaptive beamforming", IEEE Transactions on Antennas and Propagation, Vol. AP-30, No. 1, Jan. 1982.

[17] R. Monzingo and T. Miller, *Introduction to Adaptive Arrays*, John Wiley and Sons, New York, 1980.

[18] W. Rodgers and R. Compton, Jr., "Adaptive array bandwidth with tapped delay-line processing," IEEE Transactions on Aerospace and Electronic Systems, Vol. AES-15, No. 1, pp. 21-27, Jan. 1979.

[19] J. Mayhan, A. Simmons, and W. Cummings "Wide-band adaptive antenna nulling using tapped delay lines," IEEE Transactions on Antennas and Propagation, Vol. AP-29, No. 6, pp 923-936, Nov. 1981.

[20] B. Widrow, K. Duvall, R. Gooch, and B. Newman, "Signal cancellation phenomena in adaptive antennas: causes and cures," IEEE Transactions on Antennas and Propagation, Vol. AP-30, No. 3, pp 469-478, May 1982.

[21] K. Duvall, "Signal cancellation in adaptive antennas," Ph.D. dissertation, Dept. of Elec. Eng., Stanford University, June 1983

[22] J. Mayhan, "Some techniques for evaluating the bandwidth characteristics of adaptive nulling systems," IEEE Transactions on Antennas and Propagation, Vol. AP-27, No. 3, pp. 363-373, May 1979.

[23] Goodwin and Payne, *Dynamic System Identification: Experiment design and data analysis,* Academic Press, New York, 1977

[24] P. E. Mantey and L. J. Griffiths, "Iterative Least-Squares Algorithms for Signal Extraction," Proceedings of the Second Hawaii International Conference of System Sciences, pp. 767-770, 1968.

[25] B. Widrow, R. Gooch and T. AuTroung, "Research on Algorithms for Adaptive Antenna Arrays," Annual Interim Report, Rome Air Development Center, Contract No. F30602-80-C-0046, Feb. 1982

[26] J. Claerbout *"Fundamentals of Geophysical Data Processing: With Application to Petroleum Prospecting,"* McGraw Hill, 1976.

[27] R. Gooch, "Theory and applications of the equation-error approach to adaptive pole-zero signal processing," PhD Thesis, Dept. of Elec. Eng., Stanford University, June 1983.

[28] S. White, "An adaptive recursive digital filter," Conference Record, Ninth Annual Asilomar Conference on Circuits, Systems and Computers, Nov. 1975.

MISSION
of
Rome Air Development Center

RADC plans and executes research, development, test and selected acquisition programs in support of Command, Control Communications and Intelligence (C^3I) activities. Technical and engineering support within areas of technical competence is provided to ESD Program Offices (POs) and other ESD elements. The principal technical mission areas are communications, electromagnetic guidance and control, surveillance of ground and aerospace objects, intelligence data collection and handling, information system technology, ionospheric propagation, solid state sciences, microwave physics and electronic reliability, maintainability and compatibility.


DAT
ILM